NAVAL POSTGRADUATE SCHOOL
Monterey, California

THESIS

PROPAGATION OF SOUND IN A FAST BOTTOM UNDERLYING
A WEDGE-SHAPED MEDIUM

by

Norine A. Bradshaw

September 1980

Thesis Advisor: A. B. Coppens

Approved for public release; distribution unlimited

81 2   13 047

REPORT DOCUMENTATION PAGE		READ INSTRUCTIONS BEFORE COMPLETING FORM
1. REPORT NUMBER	2. GOVT ACCESSION NO. AD-A094984	3. RECIPIENT'S CATALOG NUMBER
4. TITLE (and Subtitle) Propagation of Sound in a Fast Bottom Underlying a Wedge-Shaped Medium .		5. TYPE OF REPORT & PERIOD COVERED Master's Thesis, September 1980
		6. PERFORMING ORG. REPORT NUMBER
7. AUTHOR(s) Norine A. Bradshaw		8. CONTRACT OR GRANT NUMBER(s)
9. PERFORMING ORGANIZATION NAME AND ADDRESS Naval Postgraduate School Monterey, California 93940		10. PROGRAM ELEMENT. PROJECT. TASK AREA & WORK UNIT NUMBERS
11. CONTROLLING OFFICE NAME AND ADDRESS Naval Postgraduate School Monterey, California 93940		12. REPORT DATE September 1980
		13. NUMBER OF PAGES 82
14. MONITORING AGENCY NAME & ADDRESS(if different from Controlling Office) Naval Postgraduate School Monterey, California 93940		15. SECURITY CLASS. (of this report) Unclassified
		15a. DECLASSIFICATION/DOWNGRADING SCHEDULE

16. DISTRIBUTION STATEMENT (of this Report)

Approved for public release; distribution unlimited

17. DISTRIBUTION STATEMENT (of the abstract entered in Block 20, if different from Report)

18. SUPPLEMENTARY NOTES

19. KEY WORDS (Continue on reverse side if necessary and identify by block number)

acoustics
sound propagation
continental shelf
method of images

20. ABSTRACT (Continue on reverse side if necessary and identify by block number)

The pressure and phase distribution of sound in a fast fluid medium underlying a tapered fluid medium was modeled using a Green's function approach. The model predicted well-defined beams in the bottom, with apparent interference effects strongly evident for cases at a distance from the wedge interface. The effects of attenuation on the patterns were studied. A simple expression for determining the beam depression angle as a function, the wedge angle, the sound speed ratio, and the density ratio was derived. Comparisons with laboratory measurements were made.

DD FORM JAN 73 1473 EDITION OF 1 NOV 65 IS OBSOLETE
(Page 1) S/N 0102-014-6601

Propagation of Sound in a Fast Bottom Underlying
a Wedge-Shaped Medium

by

Norine A. Bradshaw
Lieutenant Commander, United States Naval Reserve
B.S., Michigan State University, 1968

Submitted in partial fulfillment of the
requirements for the degree of

MASTER OF SCIENCE IN ENGINEERING ACOUSTICS

from the

NAVAL POSTGRADUATE SCHOOL
September 1980

Author: _____

Approved by: _____
                                    Thesis Advisor

_____
                                    Second Reader

_____
Chairman, Department of Physics and Chemistry

_____
Dean of Science and Engineering

2

ABSTRACT

The pressure and phase distribution of sound in a fast fluid medium underlying a tapered fluid medium was modeled using a Green's function approach. The model predicted well defined beams in the bottom, with apparent interference effects strongly evident for cases at a distance from the wedge interface. The effects of attenuation on the patterns were studied. A simple expression for determining the beam depression angle as a function the wedge angle, the sound speed ratio, and the density ratio was derived. Comparisons with laboratory measurements were made.

TABLE OF CONTENTS

I. INTRODUCTION

The problem of radiation behavior in a wedge-shaped medium overlying a bottom possesing a greater speed of sound has been investigated both optically and acoustically. In 1971, Tien and Martin (Ref. 1) deposited a thin, tapered, dielectric film on a substrate having a higher refractive index, and observed the behavior of a laser beam coupled into the film. Perfect reflection at the film-substrate interface was observed until the changing angle of incidence decreased below the critical angle for continued mode propagation. For angles of incidence below critical, the light was converted into radiation modes in the substrate.

A concurrent analysis of the acoustic problem was done by Kuznetzov (Ref. 2). Kuznetzov developed a theory, based on normal-modes, that predicted the following for sound propagating within a wedge-shaped medium overlying a half-space with a higher sound speed:

1. As the sound approached the vertex of the wedge, it would continue to be totally reflected until the angle of incidence decreased to the limiting angle of total reflection.

2. Sound incident at less than the limiting angle of total reflection would be totally refracted into the underlying half-space. This refraction occurs within the region from the wedge apex to the point where the limiting angle was attained.

6

3. Within the half-space, the acoustic energy would be propagated as a well defined beam with the maximum pressure amplitude occurring at an angle of depression from the wedge interface within the range β to 2β, where β is the wedge angle.

Kuznetzov also performed a series of experiments that supported his theory.

Subsequent optical experiments by Tien, Smolinsky, and Martin (Ref. 3) demonstrated the formation of a well-defined beam within the substrate. The accompanying theoretical discussion predicted conflicting behavior. Ray-optics predicted refraction into the substrate after the cutoff distance (the point where refraction begins) and wave theory predicted complete refraction into the substrate before the cutoff point. Sigelman, et. al. (Ref. 4) both predicted and observed a well columnated beam in a water-aluminum wedge system, but the observed beam was much broader than predicted. Also, the pressure maxima for the columnated beam occurred at approximately $11°$ for a wedge angle of $1.3°$, well outside the limit predicted be Kuznetzov.

The primary objective of this theoretical development is to produce a simple, fast computer model to predict the pressure and phase distribution of the columnated sound beam in the fast substrate. The pressure and phase distribution along the wedge interface calculated by Kawamura (Ref. 5) will be used as input to the substrate model, and will specifically be used as the boundary conditions for a Green's function analysis. To remove explicit frequency dependence, all relevant distances will be normalized to the distance measured from the apex along the wedge interface at which the critical reflection angle is first exceeded; this dump

distance is referred to as the dump distance X. Integration over the

wedge interface will be truncated at distances sufficient to encompass

only selected modes of interest. Results will be analyzed for trends

and compared with existing measured data.

II. THEORY

Pressure and phase distributions along the bottom of a wedge-
shaped medium are obtained using an adaptation of the method of images
as prescribed in Ref. 5. The source may be set at either finite or
infinite distance, but must be maintained sufficiently far from the
wedge boundaries to ensure that impinging waves are essentially locally
planar. The following theoretical discussion uses the above pressure
and phase distribution as initial conditions, and calculates the
pressure and phase distribution in the fast bottom by utilizing the
Green's function (Ref. 6).

Figure II-1 illustrates the geometry of the problem. The horizontal
x-axis and the vertical z-axis have their point of origin at the wedge
apex, with the positive x-axis forming the interface between the wedge
and fast bottom. The wedge angle is designated β and the angle
specifying the sound source location is δ. X is the first mode
dumping distance, and is a distance determined as follows:

$$\theta_c = \arccos (C_2 / C_1) \qquad\qquad (II-1a)$$

$$D_0 = C_1 / \{ 4 \cdot f \cdot \sin(\theta_c) \} \qquad\qquad (II-1b)$$

$$X = D_0 / \sin(\beta) \qquad\qquad (II-1c)$$

-X

Field Point

$\sigma = |\vec{r}|$

$z, \iota_1 = z/X$

θ_K

$\vec{r}'$

O

ϕ

β

$\rho_0 = 0, C_0 = 0$

Source

ρ_1, C_1

$x, \xi = x/X$

ρ_2, C_2

$C_2 > C_1$
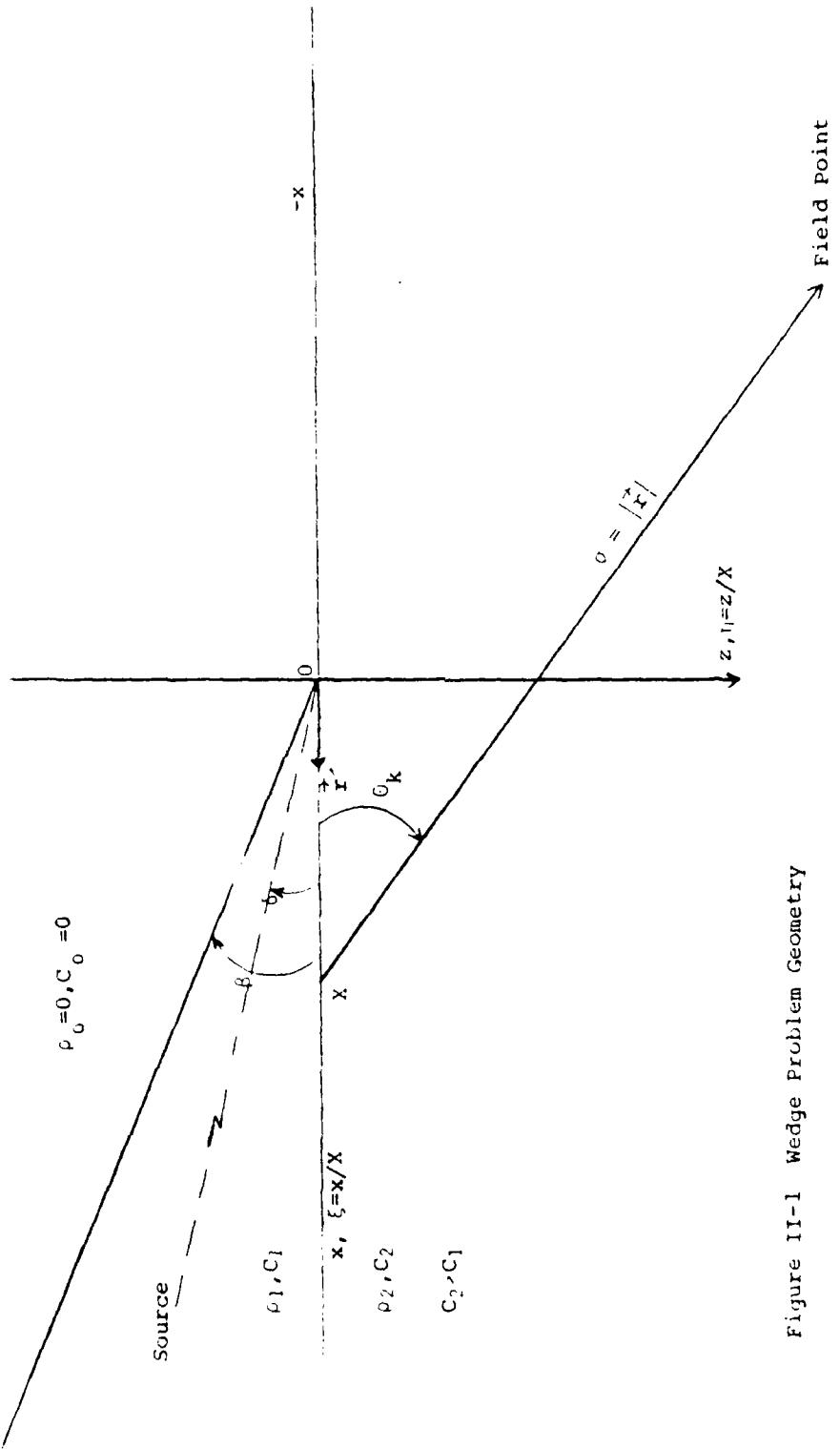
Figure II-1 Wedge Problem Geometry

10

where

C_1 = sound speed in the wedge

C_2 = sound speed in the bottom

f = frequency

and D_o = lowest mode cut-off depth.

To make the problem frequency independent, all distances were

normalized to X by defining

$$\xi = x \, / \, X \tag{II-2a}$$

$$\xi' = x' \, / \, X \tag{II-2b}$$

and
$$\eta = z \, / \, X \tag{II-2c}$$

The variable x' is identical to x, and ξ' is identical to ξ. The

prime designation is required for dummy variables of integration in

the Green's function development to follow.

Pressure along the wedge bottom is then given by

$$p(\xi, \eta=0, t) = P(\xi) \, \exp \{i[\omega t + L(\xi)]\} \tag{II-3}$$

where $P(\xi)$ is the pressure amplitude along the wedge bottom and $L(\xi)$

is the phase along the wedge bottom. Pressure in the bottom, away

from the boundary, is then given by Ref. 7,

$$p(\vec{r}, t) = \exp[i\omega t] \frac{1}{4\pi} \int_o^\infty P(\xi') \left. \frac{\partial G}{\partial z'} \right|_{z'=0} X \, d\xi' \tag{II-4}$$

$$\equiv \exp\left[i\omega t\right] R(\vec{r})$$

where G is the appropriate Green's function. The z' coordinate is identical to the z coordinate and $\vec{r} = (\vec{x}^2 + \vec{z}^2)^{\frac{1}{2}}$. The appropriate Green's function, for a line source in cylindrical geometry is

$$G(\vec{r},\vec{r}') = i\pi H_2^{(2)} (k_2|\vec{r} - \vec{r}'|) \qquad (II-5)$$

where k_2 is the propagation vector in the bottom and $\vec{r}' = \left[(\vec{x}')^2 + (\vec{z}')^2 \right]$. Differentiation of the Green's function yields (Ref. 7)

$$\frac{\partial G}{\partial z'} = i\pi H_2^{(2)} (k_2|\vec{r} - \vec{r}'|) \frac{k_2(z - z')}{|\vec{r} - \vec{r}'|} \qquad (II-6)$$

where $k_2|\vec{r} - \vec{r}'| \gg 2\pi$ and $H_0^{(2)}$, $H_1^{(2)}$ are zero and first order Bessel functions of the third kind (Hankel functions) respectively. Using equations (II-2a,b,c) at $z' = 0$ the expression $|\vec{r} - \vec{r}'|$ may be rewritten as

$$|\vec{r} - \vec{r}'| = X \left[(\xi - \xi')^2 + \eta^2 \right]^{\frac{1}{2}} \qquad (II-7)$$

Substituting (II-7) into equation (II-6), and evaluating $\frac{\partial G}{\partial z'}$ at $z' = 0$ yields

$$\frac{\partial G}{\partial z'}\bigg|_{z'=0} = \frac{\pi\left(\frac{2}{\pi k_2}\right)^{\frac{1}{2}} \exp\left(\frac{i\pi}{4}\right) \exp\{-ik_2 X[(\xi-\xi')^2 + \eta^2]^{\frac{1}{2}}\}k_2\eta X}{X^{3/2}[(\xi-\xi')^2 + \eta^2]^{3/4}} \qquad (II-8)$$

Combining equations (II-8) and (II-4) yields a time independent expression for amplitude and phase, $R(\vec{r})$

$$R(\vec{r}) = \frac{\eta}{4} \exp\left(\frac{i\pi}{4}\right)\left(\frac{2k_2 X}{\pi}\right)^{1/2}$$

$$\int_0^\infty \frac{P(\xi')\exp\{i[L(\xi')-k_2 X[(\xi-\xi')^2+\eta^2]^{1/2}]\}d\xi'}{[(\xi-\xi')^2+\eta^2]^{3/4}} \qquad (II-9)$$

Equation (II-9) is the basic equation used for the calculation of phase and amplitude in the bottom.

12

III. DEVELOPMENT OF WDGBTM

Program WDGBTM was designed to perform four main functions. First, the pressure and phase along the interface of a wedge and underlying fast media may be calculated in two ways, for both infinitely and finitely distant sound sources in accordance with Ref. 5. Modifications were made to the code of Ref. 5 to facilitate subsequent in-bottom calculations, and to enhance user flexibility. These changes did not affect results. Then using the first code as input, additional code enables both the computation of pressure and phase along a line perpendicular to the wedge bottom, and as a function of radius and angle measured from the first mode dumping point, X.

Modes of program execution may be chosen by literal input directives combined with appropriate numerical input. Appendix A illustrates an input set that utilizes all four options. Output consists of both printed listings and graphics.

Program versions exist for execution on both a CDC 6500 and an IBM 360. The CDC 6500, with a 60 bit word, does not require double precision for accuracy equivalent to the IBM 360 output. The CDC version of WDGBTM has simpler varian control routines, and separate output files for each pressure/phase variation. This enables optional *suppression* of listings. Execution time on the CDC 6500 is roughly ten times faster than on the IBM 360. For average input sets, times are 150 and 1500 cp seconds respectively.

A. EQUATION PREPARATION

1. Depth Domain

Integrations along lines perpendicular to the wedge bottom were designated depth domain calculations. The program was designed to allow specification of the field point, i.e., specification of where along the media interface line the perpendicular probe line could be dropped. The field point is not confined to lines directly beneath the wedge, but may extend to points beyond the wedge apex. These points would be values of negative x in Figure II-1. The beginning and ending points of the section of the perpendicular to be examined, and the number of field points used in the interval were also to be specified.

Equation (II-9) was split into real and imaginary components before coding. Integration order selected was over the entire ξ' domain for each η point.

2. Angle Domain

Examination of Figure II-1 verifies the following geometric relationships.

$$\varepsilon = \sigma \, \cos\Theta_k \qquad (III\text{-}1a)$$

and

$$\eta = (\sigma^2 - \varepsilon^2)^{1/2} \qquad (III\text{-}1b)$$

where ε is the distance from X to the ξ' coordinate of the field point of interest and σ is the radial distance from X to the field point.

14

Substitution of equations (III-1a) and (III-1b) into equation (II-9) yields

$$R(\vec{r}) = \frac{(\sigma^2 - \varepsilon^2)^{1/2}}{4} \, exp\left(\frac{i\pi}{4}\right) \left(\frac{2k_2 X}{\pi}\right)^{1/2} \qquad (III-2)$$

$$\int_0^\infty \frac{P(\xi') exp\{i[L(\xi') - k_2 X[(\xi-\xi')^2 + \sigma^2 - \varepsilon^2]^{1/2}]\} d\xi'}{[(\xi-\xi')^2 + \sigma^2 - \varepsilon^2]^{3/4}}$$

Equation (III-2) is the basis for angle domain calculations. The specification of σ originating at X was chosen to conform to existing experimental data (Reference 8). The length of the radius, the beginning and ending of the angular sweep, and the angular increment comprise the input specifications. As in the depth domain option, equation (III-2) was split into real and imaginary components before coding.

3. Design Restrictions

Theoretical development of program WDGBTM assumes the sound source is sufficiently distant to ensure essentially locally planar waves at the interface and the in-bottom measurements satisfy the condition $k_2 \, |\vec{r} - \vec{r}'| >> 2\pi$.

4. Program Results

An initial set of WDGBTM runs were made in the depth domain for a perpendicular directly down from the wedge apex. The source was infinitely distant and set at an angle of $\beta/2$. This limited modes within the wedge to odd numbered (symmetric) modes only. Integration over the wedge bottom was truncated at ξ equal four, so that only modes one and three were considered as contributing significantly to the beam pattern in the bottom. *Beam patterns in the bottom were calculated over the range* η *equal zero to 1.3X.*

15

The initial set was comprised of seventy-five runs. In addition

to the above criteria, the runs were generated by all possible combi-

nations of the following specifications. The ration ρ_1/ρ_2 was 0.95,

0.90, 0.80, 0.70 or 0.50. The sound speed ratio, C_1/C_2 was set at 0.95,

0.90, or 0.85. The wedge angle β was varied through 10, 6.92, 5, 2 and

1 degree(s).

From the results of the initial data set, the depression angle and

beam width was calculated for the beam pattern in the bottom. Results

are summarized in Appendix B. These results were then used to find a

simple analytical formula to predict the depression angle as discussed

in Section IV.

Other runs were made for perpendiculars at $x = -9X$ from the wedge

apex. These runs displayed apparent strong interference phenomona and

are discussed in detail later.

Angle domain executions were made to compare with experimental data.

Results are discussed in Section VII.

B. SENSITIVITY TO INTEGRATION STEP SIZE

It was desirable to keep both the integration step size and the field

point increment size as large as possible in order to minimize total

computer resources required. Increment of 0.01 times the dump distance

(X) proved to be optimum for both integration increments along the

wedge interface and field point steps in the bottom.

To illustrate the adequacy of 0.01X increment, a series of runs were

made in accordance with Table III-1. An overlay of wedge interface

pressure amplitude for $\Delta x = 0.01X$ and $\Delta x = 0.001X$ demonstrated no dis-

tinguishable difference. Likewise, depth domain plots (a, b, c, d of

16

Table (III - 1)

Sensitivity to Integration Step Size (Δx) and Field point interval size ($\Delta \eta$)

$$\Delta x = 0.001 \qquad\qquad \Delta x = 0.0001$$

$\Delta\eta=0.01$ $\Delta\eta=0.001$ $\Delta\eta=0.01$ $\Delta\eta=0.001$

(a)   (b)   (c)   (d)
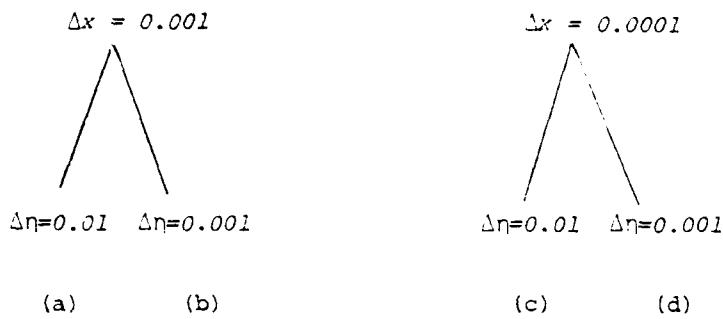
Run	η amp max	ϑ_D
a	0.240	13.50
b	0.244	13.71
c	0.240	13.50
d	0.243	13.66

Table III-1) could be identically superimposed. Use of an integration
step size of 0.001X resulted in a calculated depression angle within
one percent of the depression angle for the 0.01X run. Utilization of
a step size of greater than 0.01X is not recommended. Within this
limitation the integrations can be carried out over 10X along the inter-
face for a maximum field interval of 10X in the bottom. The 10X re-
striction is imposed by program array size. (For the 3's specified, 0.5
degrees in the angle domain was slightly finer than the 0.01X field
point step size in the depth domain and was the field point increment of
choice).

IV. BEAM DEPRESSION ANGLE ANALYSIS

A simple relationship was sought between the physical parameters associated with the wedge system and the resultant beam.
Assume

$$\theta_{DC} \propto \beta^n \qquad (IV-1)$$

where θ_{DC} is the beam depression angle and β is the wedge angle. For each c_1/c_2 and C_1/C_2 , θ_{DC} vs β was graphed on log-log paper, and the slope (n) was measured. Results are listed in Table 1 of Appendix C, n equals 0.329.

Then θ_{DC} was found as a function of C_1/C_2. The critical angle, θ_c, is an explicit function of C_1/C_2

$$\theta_c = arccos\ (C_1/C_2)\ ,\theta_c\ \text{in radians} \qquad (IV-2)$$

It was then assumed

$$\theta_{DC} \propto \beta^{0.329}\ \theta_c^{\ M} \qquad (IV-3)$$

For any constant β, M was derived as the slope of a log-log graph of θ_{DC} vs θ_c. Graphs were analysed for β equal to 10, 6.92, 5, 2 and 1 degree, and c_1/c_2 ratios of 0.95, 0.90, 0.85, 0.70 and 0.50. Results are summarized in Table (2) of Appendix C, $M = 0.772$.

The same process was repeated for ascertaining dependence on ρ_1/ρ_2 . Log-log graphs were prepared by holding β and θ_C constant using the assumed relation

$$\theta_{DC} \propto \beta^{0.329} \; \theta_C^{0.772} \; (\rho_1/\rho_2)^q \qquad (IV\text{-}4)$$

Results are summarized in Table 3 of Appendix C. $q = -0.254$.

The proposed formula is now dependent on all physical properties, assuming the source angle is maintained at one-half β. To remove the proportionality sign, write

$$\theta_{DC} = K \; \beta^{0.329} \; \theta_C^{0.772} \; (\rho_1/\rho_2)^{-0.254} \qquad (IV\text{-}5)$$

and solve for K . From Table 4, Appendix C, $K = 17.22/\text{radian}$. Therefore

$$\theta_{DC} = 17.22 \; \beta^{0.329} \; \theta_C^{0.772} \; (\rho_1/\rho_2)^{-0.254} \qquad (IV\text{-}6)$$

where β is in *degrees* and θ_C in radians.

θ_{DC} calculated from equation (IV-6) and the difference between θ_{DC} and θ_D from program WDGBTM (labeled $\Delta\theta_D$ and θ_{DW} respectively) are also tabulated on Table 4, Appendix C. $\Delta\theta_D$ varies from a minimum of 0.00 to a maximum of 1.25, with the average of the absolute values of $\Delta\theta_D$ equal to 0.36. Errors ranged from zero percent to *5.0 percent*. Thus θ_{DC} gives a reasonable approximation of the beam depression angle.

A similar formula

$$\theta_{DA} = 17.1 \; \beta^{1/3} \; \theta_C^{0.773} \; (\rho_1/\rho_2)^{-0.27} \qquad (IV-7)$$

was developed independently by A. Coppens (Reference 6) The minimum

deviation of θ_{DA} from θ_{DW} is 0.01 and the maximum deviation is 1.56.

The average of the absolute value of the deviation is 0.36. Both

formulas are best for ρ_1/ρ_2 close to 1.0, and less accurate for

ρ_1/ρ_2 equal to 0.5.

V. THE EFFECT OF ATTENUATION

As previewed in Section III-A.4 the pressure distribution as a function of η at $x = -9.0X$ demonstrated apparent interference effects (see figure V-1). As integration over the wedge interface to 4X encompasses dumping by the first and third mode, and the third mode dumps about the point 3X vice X for the first mode, it is log a to expect attenuation effects to reduce the contribution of the more distant mode. The initial Green's function approach, equation (II-9) did not consider attenuation of the acoustic wave in the bottom medium. An attenuation term

$$exp\ \{-\alpha\left[(\xi-\xi')^2 + \eta^2\right]^{1/2}\} \tag{V-1}$$

was incorporated into equation (II-9) to yield

$$R(\vec{r}) = \eta/4\ exp\left(\frac{i\pi}{4}\right)\left(\frac{2k_2X}{\pi}\right)^{1/2} \tag{V-2}$$

$$\int_0^{\infty} \frac{P(\xi')exp\{-\alpha\left[(\xi-\xi')^2+\eta^2\right]^{1/2}\}exp\{i\left[L(\xi')-k_2X\left[(\xi-\xi')^2+\eta^2\right]^{1/2}\right]\}d\xi'}{\left[(\xi-\xi')^2+\eta^2\right]^{3/4}}$$

An appropriate code modification to the depth domain routine was made. The attenuation coefficient α was an input variable to the program.

Two sets of comparison runs were made. The first set consisted of an unattenuated control ($\alpha = 0$) and an attenuated run with α equal 1.0, with the pressure amplitude measured down from the wedge apex. The second set consisted of an unattenuated control plus runs with α set to 1.0, 0.5, 0.1, and 0.01 and the pressure measured at $x = -9.0$ from the

NPTS	2...	...	
NMDE	1...	...	...
NRAT	0.0500	CISC	0....
C1	1500.0000	FFNT	9.00
C2	1578.0000		
CMAT	0.9900		
BETA	2.50		
SHCA	1.25		
SHCD	999.00		
WINC	0.010		

Figure V-1
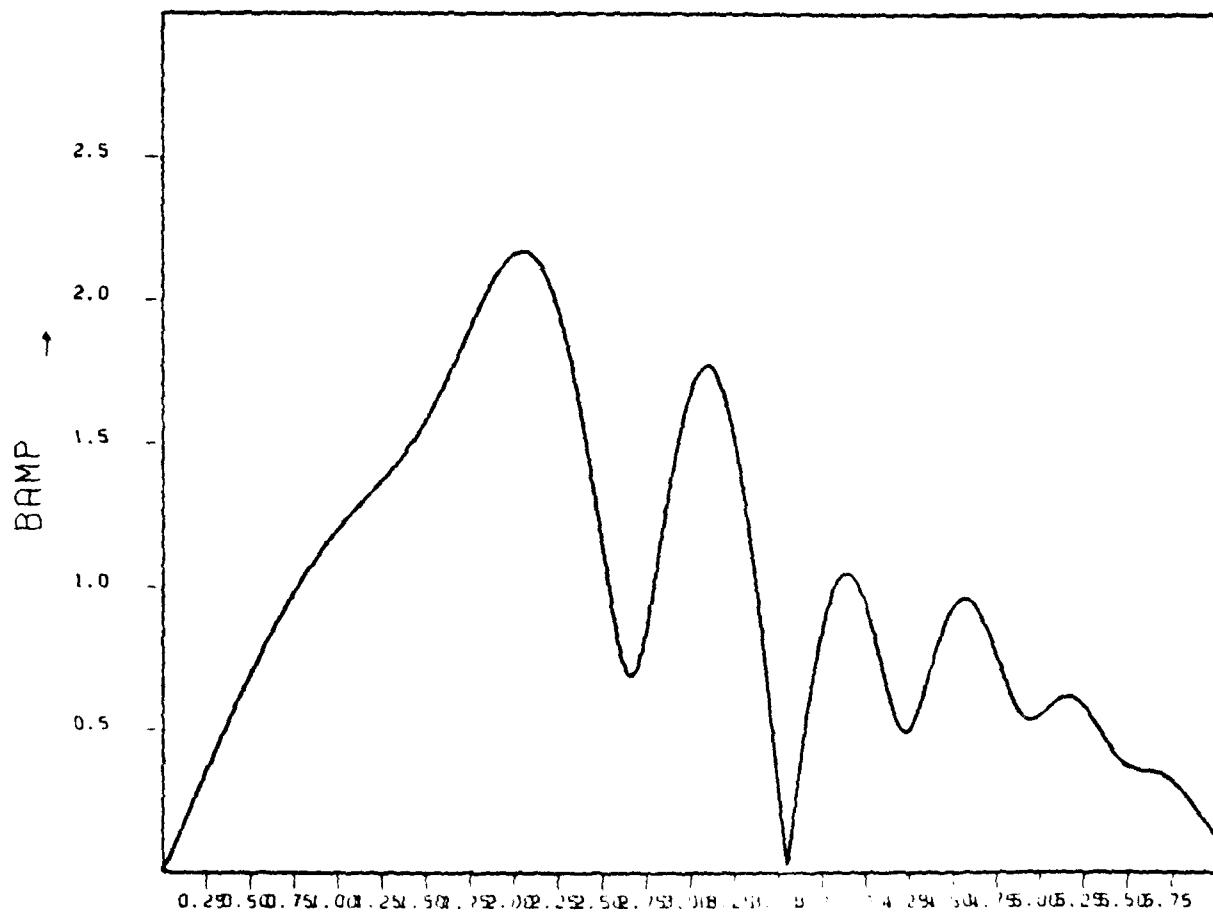
ETH

apex. All other input variables for both sets were held constant and are specified in Table (V-1). Integration over the wedge bottom was from the apex to four times the dump distance; this was to insure that contributions from the third mode (dumping about the point $x = 3X$) were included.

The results of set one are illustrated in Figure (V-2). Note that the second maxima is severely depressed in the attenuated case. The depression angle has been shifted slightly from 11.86 degrees for the unattenuated data to 11.31 degrees with α set to 1.0.

Figure V-3 is a plot of the results from set two. All curves have been normalized to the initial slope for $\alpha = 1.0$. The second and third maxima decrease with increasing α, and relatively more energy is contained in the first beam. The depression angle of the first beam decreases slightly with increasing α . These trends are summarized in Table (V-2).

Figures (V-4a) and (V-4b) illustrate the effects of attenuation on different contributing modes. For Figure (V-4a), the source was placed at 1/3 β. With this source geometry, contributions from mode three are suppressed, and only the first and second mode contributed to the beam pattern in the bottom. For Figure (V-4b), the source was placed at $\frac{1}{2}\beta$ and modes one and three propagate into the bottom medium. Both cases were run for $\alpha = 1.0$, 0.5, 0.1 and 0.0. As could be expected, attenuation causes greater suppression of third mode interference contributions than of second mode contributions.

Table (V-1)

Input Specifications for Attenuation Runs

$C_1 = 1500.0$ $\rho_1 = 1.0$

$C_2 = 1578.947$ $\rho_2 = 1.052632$

$C_1/C_2 = 0.95$ $\rho_1/\rho_2 = 0.95$

$\beta = 5.0°$ $f = 150000 \; hz$

$X_2 = 4.0$ Source distance = infinite

$\delta = 2.5°$

$\alpha = 0.0, \; 0.01, \; 0.1, \; 0.5, \; 1.0$

Refer to Figure II-1 for variable meaning.

Figure V-2

Attenuated and unattenuated pressure amplitudes
down from the apex

Figure V-3

$\alpha = 0$
$\alpha = 0.01$
$\alpha = 0.1$
$\alpha = 0.5$
$\alpha = 1.0$

$\eta \longrightarrow$
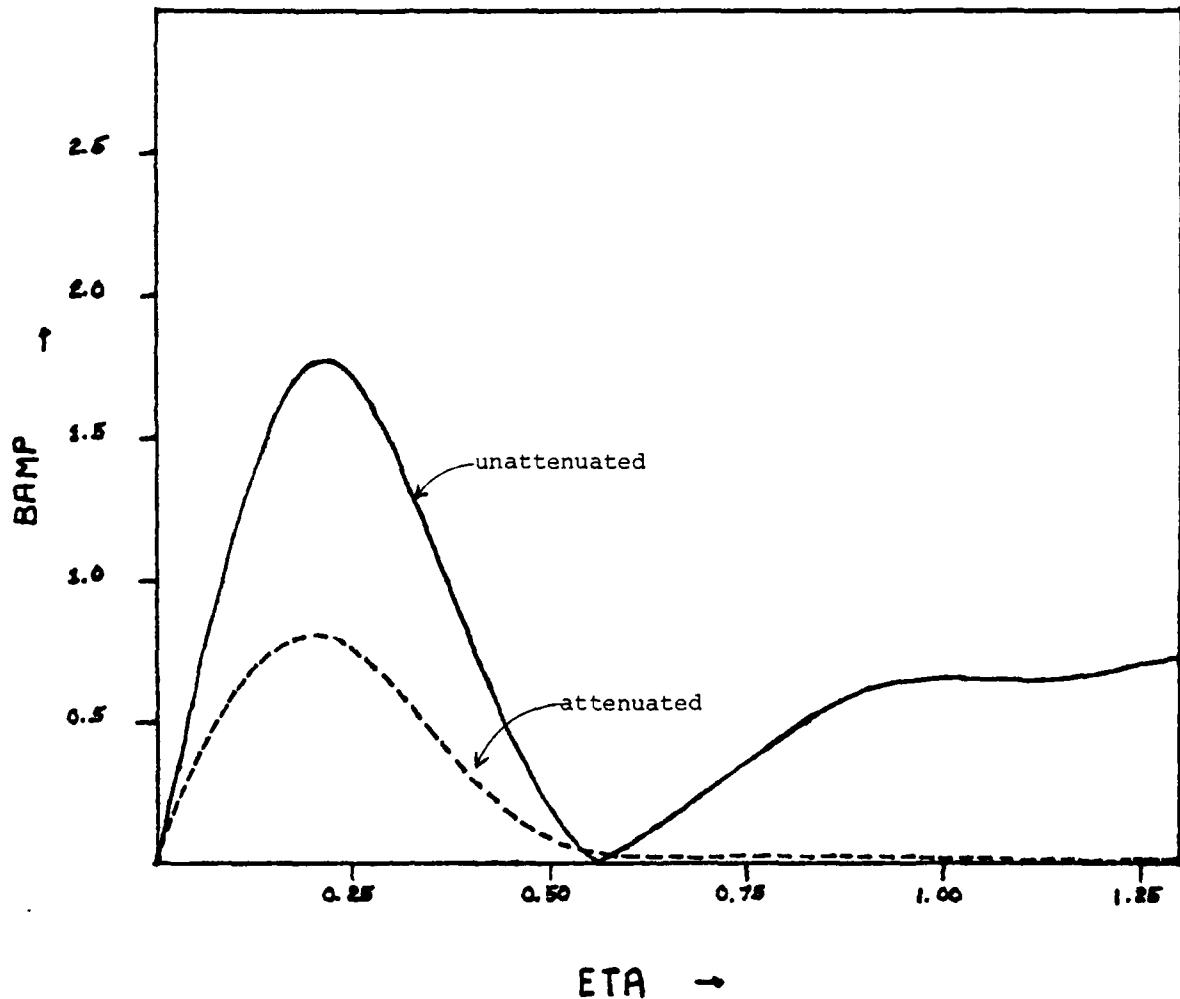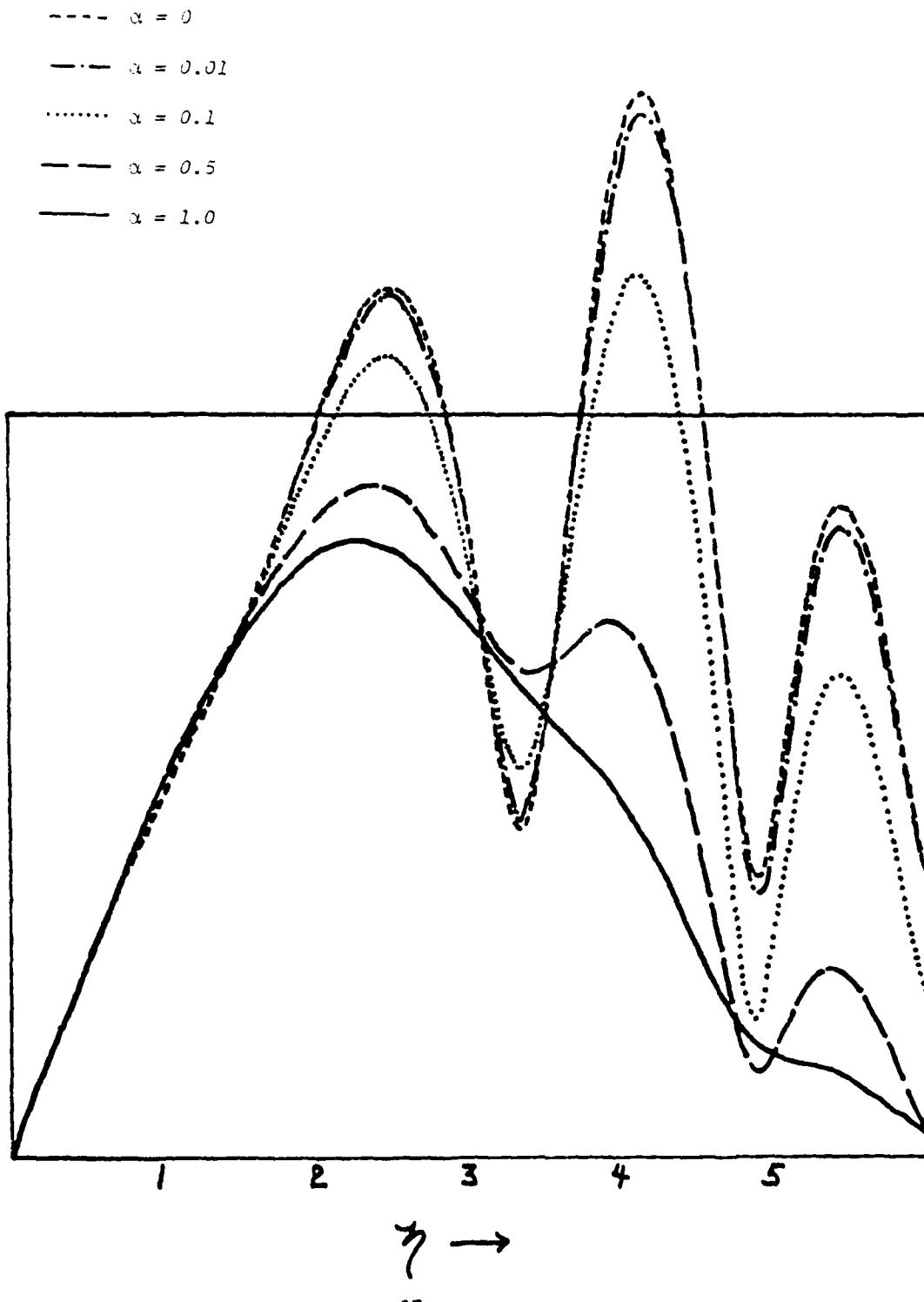
TABLE V-2

x	γ	H_1	H_2	H_1/H_2
1.0	12.84	0.21×10^{-4}	NONE	
0.5	13.39	$.33 \times 10^{-2}$	$.26 \times 10^{-2}$	1.26
0.1	13.82	0.21	0.23	0.90
0.01	13.93	0.54	0.66	0.83
0.0	13.98	0.61	0.74	0.82

γ = *depression angle of first maxima*

H_1 = *amplitude of first maxima*

H_2 = *amplitude of second maxima*

28

RHO1	0.9651	EBEG	0.0
RHO2	1.1470	EEND	4.0
RRAT	0.8415	EINC	400.
C1	1500.0000	FPNT	0.00
C2	.94.1984		
CRAT	0.8854		
BETA	1.53		
SRCA	0.51		
SRCO	999.00		
WINC	0.0,0		

Figure V-4a

α

——— 0.0

········ 0.1

– – – 0.5

–·–·– 1.0

BAMP

ETA →

RHO1   0.9651   EBEG   0.0

RHO2   1.1420   EEND   4.0

RRAT   0.8415   EINC   400.
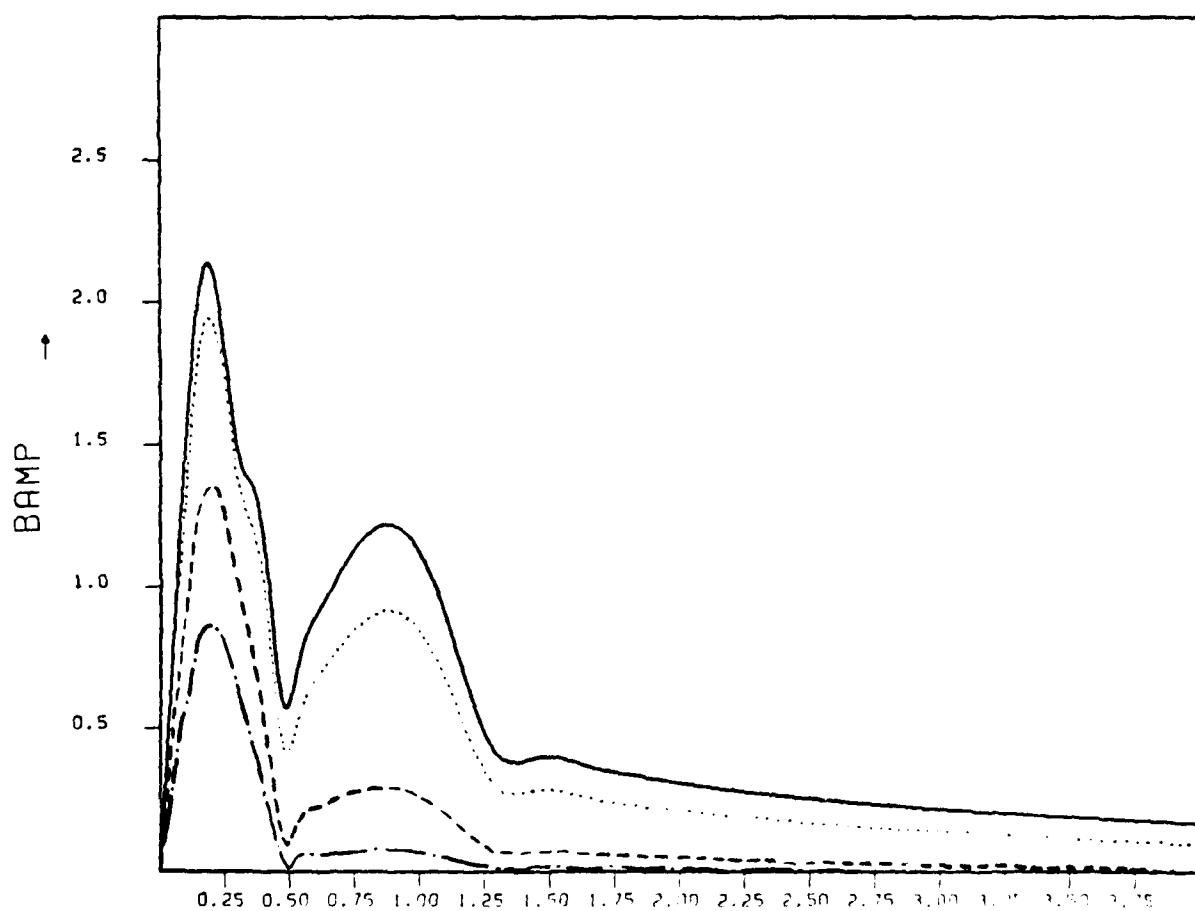
C1   1500.0000   FPNT   0.00

C2   1694.1984

CRAT   0.8854

BETA   1.53

SRCA   0.76

SRCD   999.00

WINC   0.010

Figure V-4b

χ

———— 0.0

········ 0.1

----- 0.5

—·— 1.0

30

ETA
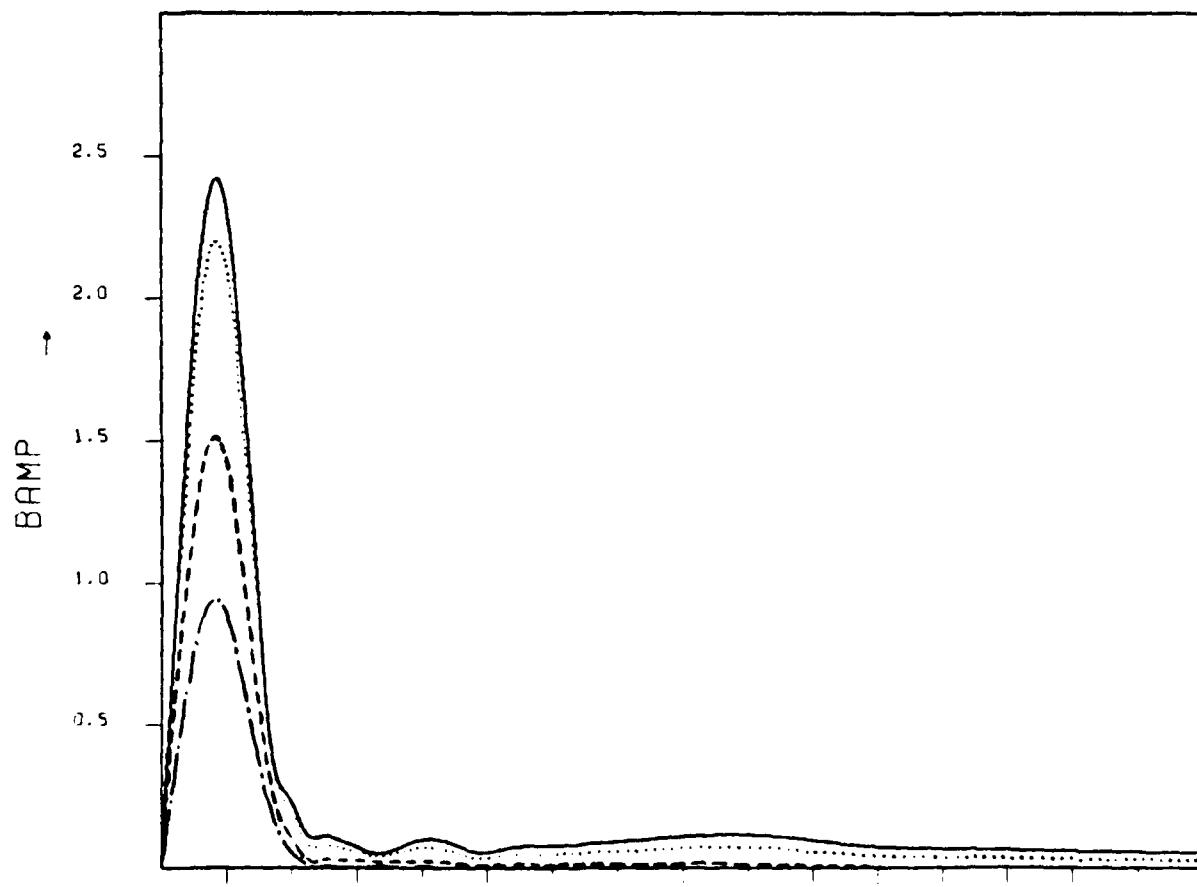
VI. ANALYSES OF FAR-FIELD INTERFERENCE PATTERNS

The results of the attenuation investigation were supportive of an interference explanation for the multiple beams. Subsequently, two analytical approaches were tried to predict the location of interference maxima and minima under unattenuated far-field conditions.

Both the Differential Change and Multiple Lambda analyses assume very simple processes. Both assume point sources of sound at the wedge interface located at X and $3X$. Reallistically the sound sources behave as phased arrays propagating assymetrically about the dumping points. Phase differences between the two dumping points are non-zero. The Differential Change formula becomes invalid as η approaches zero.

A. DIFFERENTIAL CHANGE APPROACH

Based on the simple geometric considerations illustrated in Fig $(VI-1)$, the following nondimensional formula for the change in interference maxima locations was derived.

$$\Delta\eta = \frac{4\ (C_2/C_1)\ \sin\theta_C\ \sin\beta}{\left(\frac{\eta}{[\eta^2+(1-X)^2]^{1/2}} - \frac{\eta}{[\eta^2+(3-X)^2]^{1/2}}\right)} \qquad (VI-1)$$

Note that equation (VI-1) is dependent only on the wedge angle β and the sound speeds of the two fluid media.

A series of WDGBTM executions were made for varying C_2/C_1 and β, with all other variables held constant. Table (VI-1) is a summary of one case, this case is typical of results observed. Results will be discussed in Section VI-C.

Source at 1/2 β

Figure (VI-1)

32
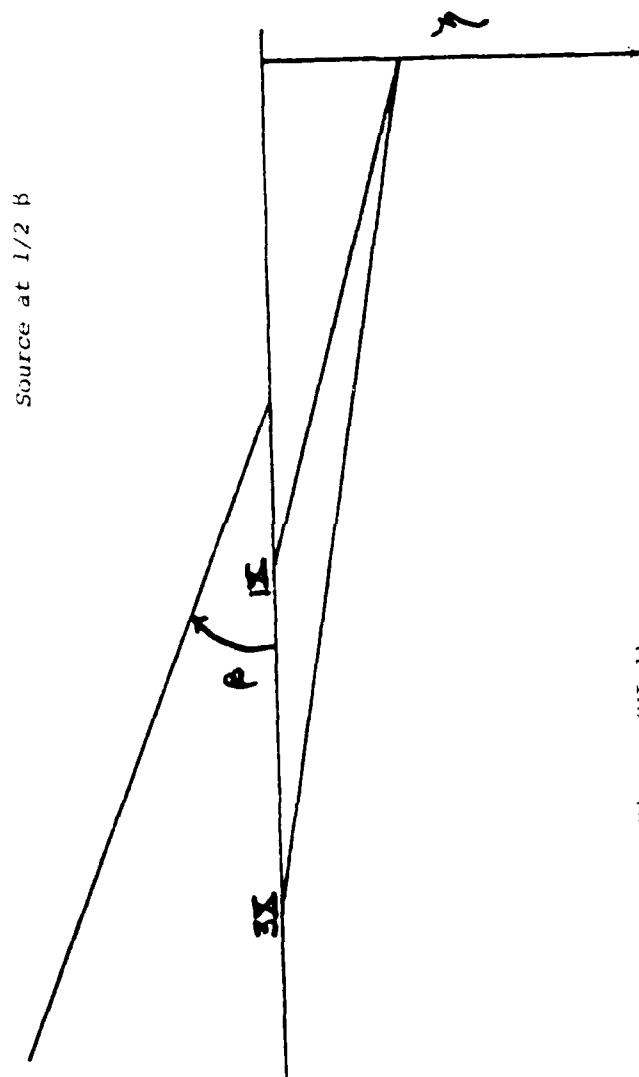
TABLE VI-1

Comparison of $\Delta\eta$ from equation (VI-1) and $\Delta\eta$ from WDGBTM results.

$$C_1/C_2 = 0.90$$

β	WDGBTM maxima locations	$\Delta\eta$ from WDGBTM	$\Delta\eta$ predicted
5.0	2.38	1.67	4.56
	4.05	1.92	3.04
	5.97		
2.5	2.33	1.40	2.33
	3.73	1.02	1.60
	4.75	0.91	1.38
	5.66		
1.25	2.08	1.22	1.29
	3.30	0.66	0.88
	3.96	0.49	0.77
	4.45		

B. MULTIPLE LAMBDA APPROACH

The second interference pattern calculation also utilizes the geometry of Fig. (VI-1). For each C_1/C_2 ratio and beta combination, X and λ_2 (the wavelength in the bottom media) was calculated according to the equations

$$X = \frac{C_1}{4f \, \sin \, \theta_C \, \sin \, \beta} \qquad \text{(VI-2)}$$

and

$$\lambda_2 = C_2/f \qquad \text{(VI-3)}$$

where   is 150khz. The ratio $\lambda_2/X = Q$
is then found and used in the relation

$$NQ = \left[\eta^2 + (3-X)^2 \right]^{1/2} - \left[\eta^2 + (1-X)^2 \right]^{1/2} \qquad \text{(VI-4)}$$

where N is any positive integer. Note that use of equation (VI-4) assumes zero initial phase.

To find the expected maxima and minima, a plot of η vs N was made for each Q. Maxima are expected for each integer N, minima for each $N + 1/2$. Table (VI-2) summarizes one case of maxima and minima expected as a result of equation (VI-4) versus maxima and minima observed on WDGBTM output.

C. SUMMARY OF ANALYSES

Predictions from both simple analyses are of the same order of magnitude as WDGBTM results. The number of maxima and minima are

TABLE VI-2

OCCURRENCE OF MAXIMA AND MINIMA

$$C_1/C_2 = 0.85$$

β (DEG)	η MAX WDGBTM	η MAX EXP	η MIN WDGBTM	η MIN EXP
5	4.03	2.68	5.39	4.70
		6.34		
2.5	3.59	2.59	4.55	3.76
	5.00	4.70	5.66	5.56
1.25	2.02	2.53	2.49	1.76
	2.35		3.56	3.16
	3.81	3.72	4.77	4.25
	5.03	4.68	5.40	5.13
	5.62	5.54	5.90	5.94

consistantly predicted as increasing with decreasing wedge angle.

Occasinal unexplainable phenomena, such as increasing WDGBTM $\ln$ for

the $\beta = 5$ on Table (VI-1) and the extra WDGBTM maxima for $\beta = 5$

Table (VI-2), were observed, but results are generally supportive of

an interference effect *occurring*.

VII. COMPARISONS

A. EXPERIMENTAL DATA

Netzorg (Reference 4) measured pressure amplitude as a function of angle for fixed radii in four media below a wedge shaped upper layer. The angle domain version of WDGBTM was used to compare calculated pressure patterns with measured patterns.

All runs utilized finite source input. For each of Netzorg's four experimental cases, corresponding computer runs were made with the source distance set to 100X, 10X and SX, where S corresponds to the actual source distance used in the tank. In all cases S was less than 10X. The integrations were carried out over one dumping distance and four dumping distances for each source.

Figure (VII-1) is typical of pressure amplitudes in the bottom. The source in the experiment was only *about* 40 wavelengths from the dumping point, even at 10X the source is approximately 110 wavelengths away. Since the method of images calculations utilized to determine the pressure amplitude along the wedge bottom assume a plane wave, it is questionable that this program can produce a realistic comparison with the measured data.

Figures (VII-2) and (VII-3) illustrate the wide variation in results obtained depending on the source distance and integration interval. Calculations demonstrate expected trends, i.e., pressure amplitude increases with decreasing radius distance (C), with closing source

Figure VII-1

RHO1	0.9651
RHO2	1.1470
RRAT	0.8415
C1	1500.0000
C2	1694.1984
CRAT	0.8854
BETA	2.51
SRCA	1.25
SRCD	1.23
WINC	0.010

- - - source at 100X

——— source at 10X

········ source at 3.5X

WAMP

CAPX
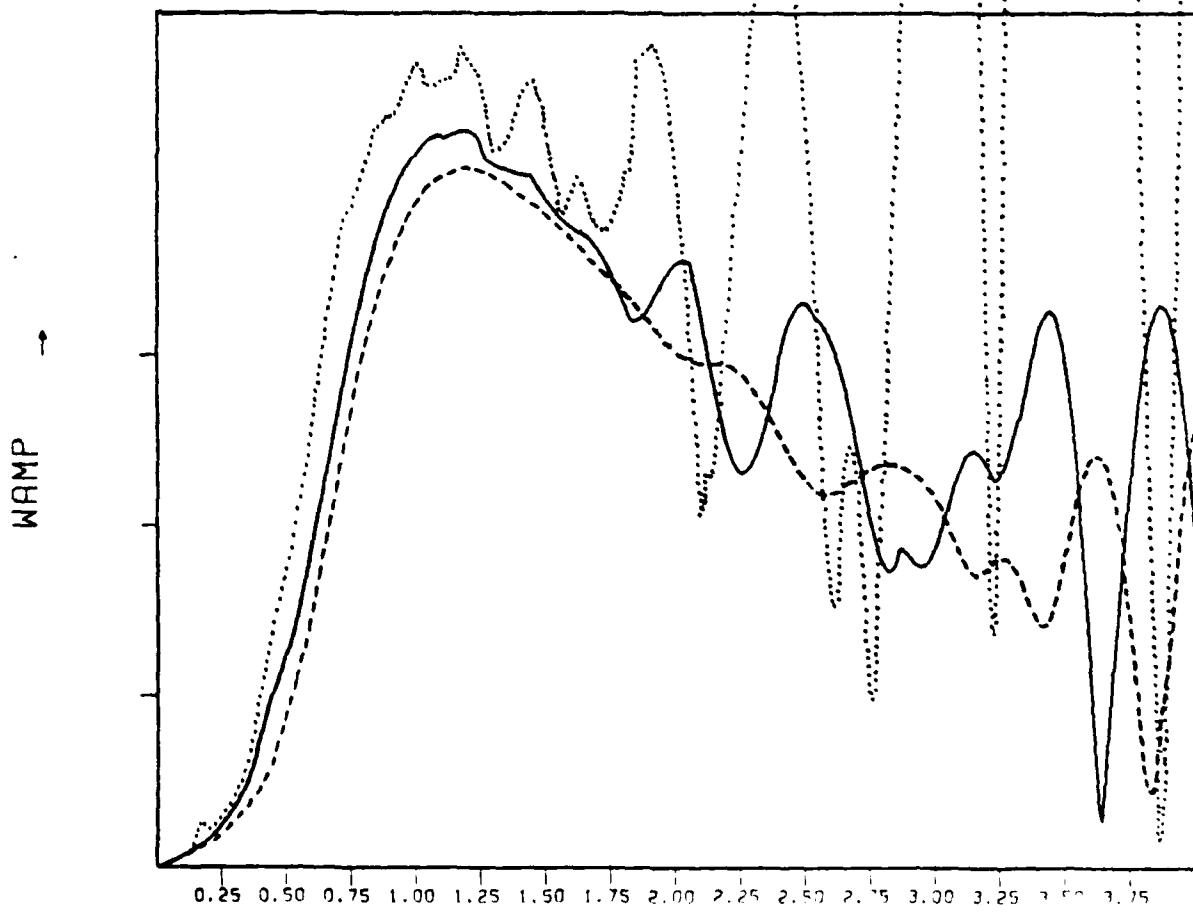
Figure VII-2

RHO1	0.9651	SGMA	1.21
RHO2	1.1470	TBEG	0.00
RRAT	0.8415	TEND	45.00
C1	1500.0000	TINC	0.500
C2	1694.1984		
CRAT	0.8854		
BETA	2.51		
SRCA	1.25		
SRCD	1.23		
WINC	0.010		

	Source Distance	X_2
—··—	3.5	1
— —	10	1
—·—	100	1
·········	3.5	4
———	10	4
———	100	4
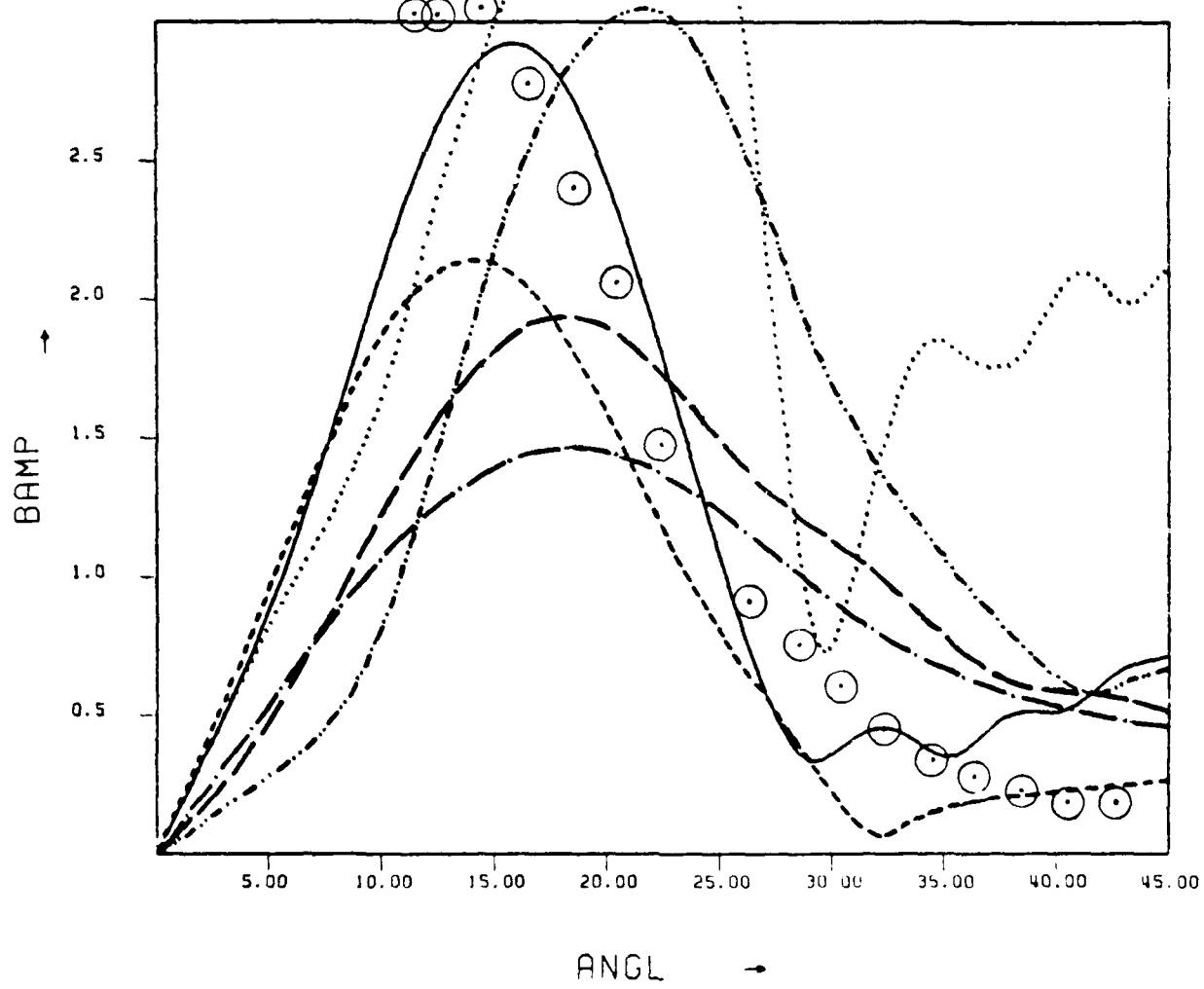
Figure VII-3
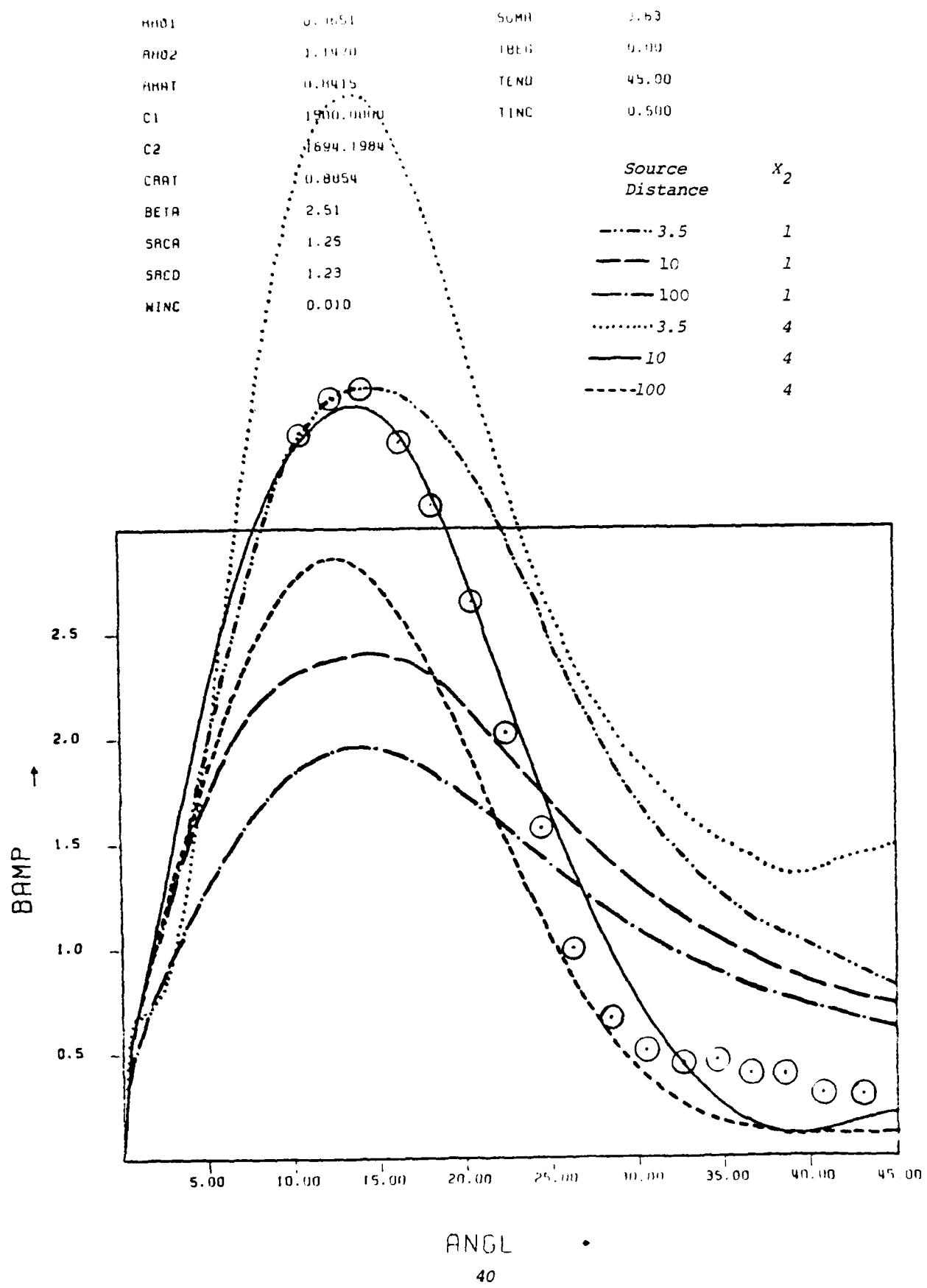
distance, and as a function of an increasing integration interval over the wedge bottom. The beam depression angle becomes more shallow as source distance increases. Results at very low angles are not considered valid because of assumptions inherent in the WDGBTM model.

The circled data points of Figures (VII-2) and (VII-3) are a transposition of data from Reference 4. Since absolute amplitude was not specified in the reference, rescaling to the case most near to the actual conditions was performed, i.e., the data were normalized to the case X_2 = 1.0 and srcd = 3.5X. The shape of the experimental curve and the apparent beam depression angle are the only valid comparisons that should be made.

Comparisons of WDGBTM beam depression angles with measured values gave varying results. Measured depression angles decreased with increasing σ, WDGBTM depression angles increased. WDGBTM results were within 6 percent to 62 percent of measured values. No correlation was observed between prediction accuracy and source distance or prediction accuracy and the interface integration interval. All measured beam depression angles in Reference ϑ were for the two shortest radii of each case, the three longer radii could only be qualitatively compared with graphical data. Possible attenuation effects were not considered. Numerical results are contained in Appendix D.

B. PARABOLIC EQUATION APPROACH

Kuperman (Reference 9) describes a Parabolic Equation model result for a wedge problem, and compares these results to one set of data extracted from Reference 10.

41

The Parabolic Equation results show very well defined beams in the bottom, with no apparent interference effects as observed in comparable WDGBTM runs (Figures V-1 and V-4). Kuperman used an attenuation factor of $0.5dB$ per wave length, a value equivalent to an input of 0.984 Nepers/X for WDGBTM. It should be noted in Figure V-4 that there is complete separation of the beams for WDGBTM when $\alpha = 1.0$.

Kuperman states agreement within 20 percent of a measured data set of Reference 10. This measured data is identical to Case 1 of Appendix D. WDGBTM accuracy for this case varied from zero percent error to 22 percent error with error calculated according to the formula

$$100 \times \frac{(\text{observed data}) - (\text{measured data})}{\text{measured data}}$$

VIII. CONCLUSIONS

1. Program WDGBTM offers a fast, efficient means of analysing the behavior of sound in a fast bottom underlying a wedge-shaped medium. Effects of attenuation are easily demonstrated, and modes desired are readily controlled by specification of source location and integration interval selected. Results of the model are not inconsistant with current measured data, and illuminate observations generated by the Parabolic Equation model.

2. A simple equation for calculating beam depression angle as a function of wedge characteristics was obtained which offers sufficient accuracy for use as a rapid analytical tool. The equation was derived for acoustic sources placed at one-half the wedge angle. Accuracy degrades when the wedge medium density to bottom medium density ratio decreases to 0.5.

3. It is recommended that further experiments be performed that would further test the model. New experiments should be sufficiently large scale to ensure plane waves at the wedge bottom interface and to *satisfy the* $k_2|\vec{r}-\vec{r}'|>>2\pi$ criteria. Bottom media that reasonably model real ocean fluid-like bottom are also recommended.

SAMPLE INPUT SET

```
INFINITE SOURCE INPUT
1500.0    1578.94737    1.00000.     1.0526315    5.0
0.0       4.0           150000.      2.5
0.400
DEPTH DOMAIN INPUT
0.0       6.00          -9.0                      600
0.100
DEPTH DOMAIN INPUT
0.010     6.00          -9.0                      600
FINITE SOURCE INPUT
1500.0    1628.0        0.98666      1.08742       2.66
0.0       4.0           150000.      1.33
0.400
10.0
ANGLE DOMAIN INPUT
1.31      0.0   45.0     0.5
ANGLE DOMAIN INPUT
0.90      0.0   45.0     0.5
DEPTH DOMAIN INPUT
0.0       1.3           0.0                        130
0.000
```

Key on following page

Key to Input Set

Line #	Value	Format
1	Literal string for infinite source option	A4
2	C_1, C_2, ρ_1, ρ_2, β,	5F15.0
3	ξ_1, ξ_2, f, δ,	4F15.0
4	number of increments for $\xi_2 - \xi_1$	I4
5	Literal string for depth domain option	A4
6	η_1, η_2, ξ, number of increments between $\eta_2 - \eta_1$	3(F15.7, 5X), I5
7	α	F15.7
8	see line 5	
9	see line 6	
10	see line 7	
11	Literal string for finite source option	A4
12	see line 2	
13	see line 3	
14	see line 4	
15	source distance in X	F15.7
16	Literal string for angle domain input	A4
17	σ, θ_{k1}, θ_{k2}, $\Delta\theta_k$	4(F5.2, 5X)
18	see line 16	
19	see line 17	
20	see line 5	
21	see line 6	
22	see line 7	

45

APPENDIX B

$$\rho_1/\rho_2 = .9500$$

c_1/c_2	β (DEG)	∢DEPRESSION	BANDWIDTH	RATIO
0.95	10.00	15.64	22.93	0.68
	6.92	13.50	19.08	0.71
	5.00	12.02	17.48	0.69
	2.00	9.09	12.19	0.74
	1.00	7.58	9.54	0.79
0.90	10.00	19.80	29.07	0.68
	6.92	17.74	26.66	0.67
	5.00	16.33	21.85	0.75
	2.00	11.31	16.20	0.70
	1.00	9.09	12.73	0.71
0.85	10.00	24.37	36.02	0.68
	6.92	21.16	31.05	0.68
	5.00	18.42	26.61	0.69
	2.00	13.50	19.45	0.69
	1.00	11.31	14.36	0.79

$∢_{DEPRESSION}$ = ARCTAN(Z/X) AT MAX AMPLITUDE

BANDWIDTH = AECTAN($Z/X_{\frac{1}{2}u} - Z/X_{\frac{1}{2}L}$)

MEAM $\dfrac{∢_D}{BW}$ = .73

46

$$\rho_1/\rho_2 = .9000$$

C_1/C_2	β (DEG)	$\measuredangle$ DEPRESSION	BANDWIDTH	RATIO
0.95	10.00	15.64	22.68	0.69
	6.92	13.49	19.08	0.71
	5.00	12.02	17.43	0.69
	2.00	9.09	12.19	0.74
	1.00	7.58	9.54	0.79
0.90	10.00	19.80	29.77	0.66
	6.92	18.42	26.75	0.69
	5.00	16.33	21.80	0.75
	2.00	12.02	15.53	0.77
	1.00	9.09	12.90	0.70
0.85	10.00	24.37	36.28	0.67
	6.92	21.16	31.22	0.68
	5.00	18.42	26.93	0.68
	2.00	13.50	19.70	0.68
	1.00	11.31	14.95	0.76

47

$$\rho_1/\rho_2 = .8000$$

C_1/C_2	β(DEG)	$\measuredangle$ DEPRESSION	BANDWIDTH	RATIO
0.95	10.00	16.33	22.39	.73
	6.92	14.20	19.19	.74
	5.00	12.79	17.33	.74
	2.00	9.82	12.13	.81
	1.00	7.58	9.87	.77
0.90	10.00	20.46	31.00	.66
	6.92	19.14	26.93	.71
	5.00	16.33	21.90	.74
	2.00	12.02	16.38	.73
	1.00	9.82	12.95	.76
0.85	10.00	25.03	36.94	.68
	6.92	22.44	31.72	.71
	5.00	19.14	27.65	.69
	2.00	14.20	20.10	.71
	1.00	11.31	15.32	.74

$$\rho_1/\rho_2 = .7000$$

c_1/c_2	β (DEG)	$\measuredangle_{\text{DEPRESSION}}$	BANDWIDTH	RATIO
0.95	10.00	17.07	22.24	.77
	6.92	14.20	19.34	.73
	5.00	13.50	17.17	.79
	2.00	9.82	12.13	.81
	1.00	8.36	9.65	.87
0.90	10.00	21.16	32.66	.65
	6.92	19.80	26.93	.74
	5.00	17.07	22.00	.78
	2.00	12.79	16.59	.77
	1.00	10.59	13.12	.81
0.85	10.00	25.64	37.88	.68
	6.92	23.12	32.29	.72
	5.00	19.80	28.72	.69
	2.00	14.95	20.56	.73
	1.00	12.02	15.85	.76

$$\rho_1/\rho_2 = .5000$$

c_1/c_2	β (DEG)	ΔDEPRESSION	BANDWIDTH	RATIO
0.95	10.00	17.74	22.73	0.78
	6.92	15.64	19.80	0.79
	5.00	14.95	16.91	0.88
	2.00	9.82	12.68	0.77
	1.00	9.09	10.26	0.89
0.90	10.00	22.44	35.53	0.63
	6.92	21.80	27.16	0.80
	5.00	18.42	23.70	0.78
	2.00	14.20	17.64	0.80
	1.00	11.31	13.87	0.82
0.85	10.00	27.20	42.80	0.64
	6.92	25.03	34.33	0.73
	5.00	21.80	31.00	0.70
	2.00	17.07	21.40	0.78
	1.00	13.50	16.91	0.80

APPENDIX C

TABLE 1

ρ_1/ρ_2	C_1/C_2	n
0.95	0.95	0.318
0.95	0.90	0.347
0.95	0.85	0.341
0.90	0.95	0.318
0.90	0.90	0.335
0.90	0.85	0.339
0.80	0.95	0.328
0.80	0.90	0.328
0.80	0.85	0.343
0.70	0.95	0.318
0.70	0.90	0.303
0.70	0.85	0.343
0.50	0.95	0.339
0.50	0.90	0.314
0.50	0.85	0.314

Average n = 0.329

Standard (N-1) deviation = 0.014

(N-1) Variance = 0.002

51

TABLE 2

c_1/c_2	S	M
0.95	10.0	0.834
0.95	6.92	0.845
0.95	5.00	0.783
0.95	2.00	0.739
0.95	1.00	0.752
0.90	10.0	0.815
0.90	6.92	0.818
0.90	5.00	0.782
0.90	2.00	0.735
0.90	1.00	0.720
0.80	10.0	0.791
0.80	6.92	0.839
0.80	5.00	0.767
0.80	2.00	0.686
0.80	1.00	0.750
0.70	10.0	0.730
0.70	6.92	0.892
0.70	5.00	0.701
0.70	2.00	0.778
0.70	1.00	0.697
0.50	10.0	0.786
0.50	6.92	0.881
0.50	5.00	0.693
0.50	2.00	1.051*
0.50	1.00	0.722

*Rejected data point   Average M = 0.772

Standard (N-1) deviation = 0.059

Variance = 0.003

52

Table 3

C_1/C_2	θ_C(rad)	β	q
0.95	0.318	10.0	-0.217
0.95	0.318	6.92	-0.285
0.95	0.318	5.00	-0.257
0.95	0.318	2.00	-0.215
0.95	0.318	1.00	-0.283
0.90	0.451	10.0	-0.183
0.90	0.451	6.92	-0.232
0.90	0.451	5.00	-0.211
0.90	0.451	2.00	-0.300
0.90	0.451	1.00	-0.317
0.85	0.555	10.0	-0.162
0.85	0.555	6.92	-0.242
0.85	0.555	5.00	-0.255
0.85	0.555	2.00	-0.362
0.85	0.555	1.00	-0.283

Average q = -0.254

standard (N-1) deviation = 0.053

variation = 0.0028

Table 4

ρ_1/ρ_2	c_1/c_2	β	θ_{DW}	K	θ_{DC}	$\Delta\theta_D$
0.95	0.95	10.0	15.64	17.54	15.35	-0.29
0.95	0.95	6.92	13.50	17.08	13.60	0.10
0.95	0.95	5.00	12.02	16.94	12.22	0.20
0.95	0.95	2.00	9.09	17.32	9.04	-0.05
0.95	0.95	1.00	7.58	18.14	7.20	-0.38
0.95	0.90	10.0	19.80	16.94	20.12	0.32
0.95	0.90	6.92	17.74	17.13	17.83	0.09
0.95	0.90	5.00	16.33	17.55	16.02	-0.31
0.95	0.90	2.00	11.31	16.43	11.85	0.54
0.95	0.90	1.00	9.09	16.59	9.43	0.32
0.95	0.85	10.0	24.37	17.77	23.61	-0.76
0.95	0.85	6.92	21.16	17.42	20.92	-0.24
0.95	0.85	5.00	18.42	16.87	18.80	0.38
0.95	0.85	2.00	13.50	16.72	13.91	0.41
0.95	0.85	1.00	11.31	17.59	11.07	-0.24
0.90	0.95	10.0	15.64	17.31	15.56	-0.08
0.90	0.95	6.92	13.49	16.85	13.79	0.30
0.90	0.95	5.00	12.02	16.71	12.39	0.37
0.90	0.95	2.00	9.09	17.08	9.16	0.07
0.90	0.95	1.00	7.58	17.89	7.30	-0.28
0.90	0.90	10.0	19.80	16.71	20.40	0.60
0.90	0.90	6.92	18.42	17.55	18.08	-0.34
0.90	0.90	5.00	16.33	17.31	16.24	-0.09
0.90	0.90	2.00	12.02	17.23	12.02	0.00
0.90	0.90	1.00	9.09	16.36	9.56	0.47
0.90	0.85	10.0	24.37	17.53	23.94	-0.43
0.90	0.85	6.92	21.16	17.18	21.21	-0.05
0.90	0.85	5.00	18.42	16.64	19.06	0.64
0.90	0.85	2.00	13.50	16.49	14.10	0.60
0.90	0.85	1.00	11.31	17.35	11.22	-0.09

Table 4 (continued)

ρ_1/ρ_2	c_1/c_2		θ_{DW}	K	θ_{DC}	$\Delta\theta_D$
0.80	0.95	10.0	16.33	17.54	16.03	-0.30
0.80	0.95	6.92	14.20	17.21	14.20	0.00
0.80	0.95	5.00	12.79	17.25	12.76	-0.03
0.80	0.95	2.00	9.82	17.91	9.44	-0.38
0.80	0.95	1.00	7.58	17.36	7.52	-0.06
0.80	0.90	10.0	20.46	16.76	21.02	0.00
0.80	0.90	6.92	19.14	17.70	18.62	-0.52
0.80	0.90	5.00	16.33	16.80	16.54	0.21
0.80	0.90	2.00	12.02	16.72	12.38	0.36
0.80	0.90	1.00	9.82	17.16	9.86	0.04
0.80	0.85	10.0	25.03	17.47	24.67	-0.36
0.80	0.85	6.92	22.44	17.68	21.85	-0.59
0.80	0.85	5.00	19.14	16.78	19.64	0.50
0.80	0.85	2.00	14.20	16.83	14.53	0.33
0.80	0.85	1.00	11.31	16.84	11.56	0.25
0.70	0.95	10.0	17.07	17.72	16.59	-0.48
0.70	0.95	6.92	14.20	16.64	14.70	0.50
0.70	0.95	5.00	13.50	17.60	13.21	-0.29
0.70	0.95	2.00	9.82	17.31	9.77	0.05
0.70	0.95	1.00	8.36	18.51	7.78	-0.58
0.70	0.90	10.0	21.16	16.75	21.75	0.59
0.70	0.90	6.92	19.80	17.70	19.27	-0.53
0.70	0.90	5.00	17.07	16.98	17.31	0.24
0.70	0.90	2.00	12.79	17.20	12.81	0.02
0.70	0.90	1.00	10.59	17.88	10.20	-0.39
0.70	0.85	10.0	25.64	17.30	25.52	-0.12
0.70	0.85	6.92	23.12	17.61	22.61	-0.51
0.70	0.85	5.00	19.80	16.78	20.32	0.52
0.70	0.85	2.00	14.95	17.13	15.03	0.08
0.70	0.85	1.00	12.02	17.30	11.96	0.06

Table 4 (continued)

ρ_1/ρ_2	c_1/c_2	β	θ_{DW}	K	θ_{DC}	$\Delta\theta_D$
0.50	0.95	10.0	17.74	16.91	18.07	0.33
0.50	0.95	6.92	15.64	16.82	16.01	0.37
0.50	0.95	5.00	14.95	17.90	14.38	−0.57
0.50	0.95	2.00	9.82	15.89	10.64	0.82
0.50	0.95	1.00	9.09	18.48	8.47	−0.62
0.50	0.90	10.0	22.44	16.31	23.69	1.25
0.50	0.90	6.92	21.80	17.89	20.99	−0.81
0.50	0.90	5.00	18.42	16.82	18.86	0.44
0.50	0.90	2.00	14.20	17.53	13.95	−0.25
0.50	0.90	1.00	11.31	17.54	11.10	−0.21
0.50	0.85	10.0	27.20	16.85	27.80	0.60
0.50	0.85	6.92	25.03	17.50	24.62	−0.41
0.50	0.85	5.00	21.80	16.96	22.13	0.33
0.50	0.85	2.00	17.07	17.96	16.37	−0.70
0.50	0.85	1.00	13.50	17.84	13.03	−0.42

Average K = 17.22
Standard (N-1) deviation = 0.51
(N-1) variance = 0.26

APPENDIX D

Case 1

x_s	x_{max}	σ	θ_{DW}	BW_w	Measured θ_D	Measured BW
2.12	1	1.60	24.5	10.33		
	1	1.10	22.0	11.34		
	1	0.83	19.0	12.88		
	1	0.66	16.5	15.27	13.5	15
	1	0.55	14.5	18.38	15.5	15
	4	1.60	23.0	6.28		
	4	1.10	22.1	8.19		
	4	0.83	19.0	12.20		
	4	0.66	16.0	13.88	13.5	15
	4	0.55	15.0	14.71	15.5	15
10	1	1.60	17.5	19.26		
	1	1.10	16.0	20.29		
	1	0.83	16.5	20.90		
	1	0.66	13.5	22.41	13.5	15
	1	0.55	12.5	23.19	15.5	15
	4	1.60	16.0	13.85		
	4	1.10	13.5	14.96		
	4	0.83	13.0	15.36		
	4	0.66	12.0	15.67	13.5	15
	4	0.55	12.0	16.33	15.5	15
100	1	1.60	16.5	22.68		
	1	1.10	15.5	23.27		
	1	0.83	14.0	23.91		
	1	0.66	13.0	24.81	13.5	15
	1	0.55	11.5	26.00	15.5	15
	4	1.60	12.0	15.18		
	4	1.10	12.0	14.93		
	4	0.83	11.5	15.25		
	4	0.66	11.0	15.94	13.5	15
	4	0.55	10.5	16.95	15.5	15

$$C_1/C_2 = 0.8854 \qquad \rho_1/\rho_2 = 0.8415 \qquad \beta = 1.52°$$

Case 2

x_s	x_{max}	σ	θ_{DW}	BW_w	Measured θ_D	Measured BW
3.50	1	1.21	21.5	18.31		
	1	0.83	17.5	20.60		
	1	0.63	14.5	24.19		
	1	0.50	12.5	26.62	13.3	15.5
	1	0.42	10.0	27.41	14.0	14.38
	4	1.21	22.5	15.04		
	4	0.83	16.0	19.24		
	4	0.63	14.0	19.32		
	4	0.50	13.0	20.34	13.3	15.5
	4	0.42	11.5	22.75	14.0	14.38
10	1	1.21	18.0	24.19		
	1	0.83	14.5	25.13		
	1	0.63	14.5	28.69		
	1	0.50	12.0	29.56	13.3	15.5
	1	0.42	9.5	30.18	14.0	14.38
	4	1.21	16.0	16.07		
	4	0.83	14.0	17.97		
	4	0.63	14.0	20.43		
	4	0.50	12.5	22.70	13.3	15.5
	4	0.42	11.5	24.96	14.0	14.38
100	1	1.21	18.5	26.64		
	1	0.83	16.0	27.72		
	1	0.63	14.0	29.29		
	1	0.50	11.5	30.89	13.3	15.5
	1	0.42	9.5	31.55	14.0	14.38
	4	1.21	14.0	17.65		
	4	0.83	13.5	17.94		
	4	0.63	12.5	19.37		
	4	0.50	11.5	21.69	13.3	15.5
	4	0.42	11.0	23.80	14.0	14.38

$$C_1/C_2 = 0.8854 \qquad \rho_1/\rho_2 = 0.8415 \qquad \beta = 2.51°$$

Case 3

x_s	x_{max}	σ	ϑ_{DW}	BW_w	Measured ϑ_D	Measured BW
6.15	1	0.58	13.5	30.13		
	1	0.40	8.0	32.50		
	1	0.30	7.0	33.47		
	1	0.24	7.0	35.75	16.4	25.5
	1	0.20	7.5	38.56	20	21
	4	0.58	14.0	24.62		
	4	0.40	10.5	30.65		
	4	0.30	10.5	35.06		
	4	0.24	10.5	41.51	16.4	25.5
	4	0.20	11.0		20	21
10	1	0.58	14.5	24.60		
	1	0.40	12.5	30.47		
	1	0.30	11.5	35.89		
	1	0.24	11.5	41.62	16.4	25.5
	1	0.20	12.0		20	21
	4	0.58	14.5	33.94		
	4	0.40	9.0	35.10		
	4	0.30	7.5	36.04		
	4	0.24	7.5	38.04	16.4	25.5
	4	0.20	7.5	40.78	21	21
100	1	0.58	14.0	35.19		
	1	0.40	8.5	35.83		
	1	0.30	7.0	36.47		
	1	0.24	7.0	38.37	16.4	25.5
	1	0.20	7.5	40.82	20	21
	4	0.58	13.5	25.14		
	4	0.40	11.0	30.32		
	4	0.30	10.0	35.38		
	4	0.24	10.0	40.97	16.4	25.5
	4	0.20	11.0	35.02	20	21

$$C_1/C_2 = 0.8854 \qquad \rho_1/\rho_2 = 0.8415 \qquad \beta = 4.41°$$

Case 4

x_S	x_{max}	σ	θ_{DW}	BW_w	Measured θ_D	Measured BW
3.10	1	1.31	18.5	15.88		
	1	0.90	14.5	17.62		
	1	0.68	13.0	20.75		
	1	0.54	10.0	22.84	12.67	12.88
	1	0.45	8.0	24.58	14.7	13.5
	4	1.31	17.5	9.65		
	4	0.90	15.5	13.38		
	4	0.68	14.0	17.32		
	4	0.54	12.0	21.72	12.67	12.88
	4	0.45	11.0	25.21	14.7	13.5
10	1	1.21	17.0	21.32		
	1	0.90	14.0	22.55		
	1	0.68	12.0	24.35		
	1	0.54	10.0	26.14	12.67	12.88
	1	0.45	8.0	26.62	14.7	13.5
	4	1.31	14.5	13.80		
	4	0.90	13.0	15.71		
	4	0.68	12.0	17.96		
	4	0.54	11.5	20.56	12.67	12.88
	4	0.45	10.0	22.82	14.7	13.5
100	1	1.31	16.0	22.58		
	1	0.90	13.5	23.71		
	1	0.68	11.5	25.18		
	1	0.54	9.5	26.56	12.67	12.88
	1	0.45	7.5	26.76	14.7	13.5
	4	1.31	12.5	15.05		
	4	0.90	11.5	15.87		
	4	0.68	11.0	17.27		
	4	0.54	10.0	19.32	12.67	12.88
	4	0.45	9.0	21.15	14.7	13.5

$$C_1/C_2 = 0.9214 \qquad \rho_1/\rho_2 = 0.9073 \qquad \beta = 2.66°$$

```
C     WDGBTM
C
C     PROGRAM WDGBTM USES THE METHOD OF IMAGES WITH EITHER
C     AN INFINITELY DISTANT OR FINITE DISTANCE SOURCE TO
C     CALCULATE THE PRESSURE AND PHASE ALONG THE BOTTOM OF
C     A WEDGE LAYING OVER A FAST BOTTOM. THE PRESSURE AND
C     PHASE ARE OUTPUT BEFORE IN BOTTOM CALCULATIONS
C     ARE BEGUN. THE PRESSURE AND PHASE ALONG THE WEDGE
C     BOTTOM ARE THEN USED TO CALCULATE PRESSURE AND
C     AND PHASE IN THE BOTTOM AS A FUNCTION OF DEPTH FROM
C     THE WEDGE BOTTOM OR AS A FUNCTION OF ANGLE AND
C     RADIUS FROM THE FIRST MODE DUMPING POINT. THE DEPTH
C     OUTPUTS ARE RESPECTIVELY REFERRED TO AS THE DEPTH
C     DOMAIN AND ANGLE DOMAIN. ALL OUTPUT IS BOTH
C     PRINTED AND PLOTTED. ALL DIMENSIONS ARE NORMALIZED
C     TO THE DUMP DISTANCE CAPX. ALL Q VARIABLES ARE
C     SINGLE PRECISION VALUES TO FEED PLOT ROUTINES.
C
C     ALL CALCULATIONS FOR PRESSURE AND AMPLITUDE ALONG
C     THE WEDGE BOTTOM ARE AN ADAPTION OF PROGRAMS BY
C     KAWAMURA (PRESSURE ON THE INTERFACE BETWEEN A
C     CONVERGING FLUID WEDGE AND A FAST FLUID BOTTOM,
C     KAWAMURA, 4. AND IOANNOU, M.S. THESIS, NAVAL
C     POSTGRADUATE SCHOOL, MONTEREY, 1978).
C
      IMPLICIT REAL*8(A-H,O-P,R-Z),REAL*4(Q),INTEGER(I-N)
      DIMENSION PA(1001),PH(1001),YY(1001),HJFX(1001),
     *BTMDPH(1001),BTMAMP(1001),BTMPHS(1001),YNORM(1001),
     *QXLAB(3),QYLAB(2),QPLOTA(1001),QNORM(1001),QBAMP(1001)
     *QETA(1001)
      COMMON C21,RC21,BETA,WN,PI,ANGLO,F,ANGLSO
      COMMON /FINE/SREDIS,RO1,RO2,C1,C2,BETADG,Y1NORM,Y2NORM,
     *C12,RTO12,PINC,PA,PH,YY,YNORM,DY,ANGLC,CAPX,N
      COMMON /ANGLE/SIGMA,CTHBEG,CTHEND,CTHINC
      COMMON /BTM/ETABEG,ETAMAX,XI,INC
      DATA QXLAB/4HCAPX,4HHETA,4HANGL/
      DATA QYLAB/4HAMP,4HBAMP/
      DATA FINI/'FINI'/
      DATA DEPT/'DEPT'/
      DATA ANGL/'ANGL'/
C
C     READ IN DATA. TYPE OF CALCULATION IS
C     DETERMINED BY LITERAL CARDS.
C
 100  READ(5,200,END=5000) CHECK
 200  FORMAT(A4)
```

61

```
300  IF(CHECK.EQ.DEPT) GO TO 2000
     IF(CHECK.EQ.ANGL) GO TO 3000

C    INPUT MUST BE SPECIFIED TO CALCULATE
C    PRESSURE AND PHASE ALONG THE WEDGE BOTTOM.
C    READ IN INPUT AS FOLLOWS.
C
C    C1 = SOUND SPEED IN THE WEDGE
C    C2 = SOUND SPEED IN THE FAST BOTTOM
C    RO1 = DENSITY IN THE WEDGE
C    RO2 = DENSITY IN THE FAST BOTTOM
C    BETADG = THE WEDGE ANGLE (DEGREES)
C    Y1NORM AND Y2NORM THE BEGINNING AND ENDING
C    DISTANCES FROM THE APEX THAT DESIGNATE
C    THE CALCULATION INTERVAL NORMALIZED TO CAPX.
C    F = THE FREQUENCY OF INTEREST (HERTZ), CONVERTS
C    ANGLSO = THE SOURCE ANGLE (DEGREES), CONVERTS
C    TO ANGLO (RADIANS)
C    N = THE NUMBER OF Y INCREMENTS TO BE COMPUTED.
C    MINIMUM RECOMMENDED IS 100 PER CAPX.  MAXIMUM
C    ALLOWED IS 1000.
C
1000 READ(5,1000) C1,C2,RO1,RO2,BETADG
     FORMAT(5F15.0)
     PI = 4.0D0*DATAN(1.0D0)
     BETA = BETADG * PI / 180D0
1010 READ(5,1010) Y1NORM,Y2NORM,F,ANGLSO
     FORMAT(4F15.0)
     ANGLO = ANGLSO * PI / 180.0D0
1020 READ(5,1020) N
     FORMAT(I4)
     IF(CHECK.NE.FINI) GO TO 1030
     READ(5,1025) SRCDIS
1025 FORMAT(F15.7)
     CALL FINESR
     GO TO 1501
1030 CONTINUE
     SRCDIS = 0.0D0
C
C    CALCUALTE THE DUMP DISTANCE CAPX AND WRITE CAPX
C
     WRITE(6,1050) C1,C2,RO1,RO2,Y1NORM,Y2NORM,BETADG,F,ANGLSO
1050 FORMAT(//15X,'INPUT DATA',25X,'WDGBTM'//
    *    25X,'C1   =',E15.7,5X,'C2  =',E15.7//
    *    25X,'RO1  =',E15.7,5X,'RO2 =',E15.7//
    *    25X,'Y1   =',E15.7,5X,'Y2  =',E15.7//
    *    25X,'BETA=',E15.7,5X,'F   =',E15.7//
```

62

```
      *     42X,'SOURCE ANGLE=',E15.7//)

      PI = 4.0D0 * DATAN(1.0D0)

C     CONVERT ANGLES IN DEGREES TO RADIANS.
C
      BETA = BETADG * PI / 180.0D0
      ANGLO = ANGLSO * PI / 180.0D0
      ANGLC = DARCOS(C1/C2)
      HO = C1 / (4.0D0 * F * DSIN(BETA)
      CAPX = HO / DSIN(BETA)
      WRITE(6,1060) HO,CAPX
 1060 FORMAT(//,20X,'LOWEST POSSIBLE MODE CUT OFF DEPTH',9X,E15.7
      *     /20X,'DISTANCE FROM APEX  ',21X,E15.7//)

C     THE RANGE WE WILL CALCULATE PRESSURE AND
C     PHASE OVER IS GIVEN BY Y2 - Y1
C
      Y1 = Y1NORM * CAPX
      Y2 = Y2NORM * CAPX
      DY = Y2 - Y1

C     CALCULATE A SERIES OF EXPRESSIONS FOR LATER
C     USE.  WN IS THE WAVE NUMBER.
C
      WN = 2.0D0 * PI * F / C1
      C21 = C2 / C1
      RC21 = C2 * RO2 / (C1 * RO1)
      C12 = C1 / C2
      RHO12 = RO1 / RO2
      PINC = 1.0D0 / DFLOAT(N)

C     WRITE LABELS FOR WEDGE BOTTOM
C
      WRITE(6,1070)
 1070 FORMAT(//22X,'DISTANCE',17X,'NORMALIZED DISTANCE',6X,
      *     'PRESSURE AMP.',12X,'PHASE ANGLE'//)

C     CALCULATE THE PRESSURE AND PHASE AS A FUNCTION
C     OF INCREMENTED DISTANCE YY.
C
      L = N + 1
      DO 1500 I = 1,L
      DISTY = Y1 + DFLOAT(I-1) * DY / DFLOAT(N)
      YY(I) = DISTY
      YNORM(I) = DISTY / CAPX
      CALL PRESS(DISTY,PAMP,PHAS)
      PA(I) = PAMP
      PH(I) = PHAS
```

63

```
      WRITE(6,1550) YY(I),YNORM(I),PA(I),PH(I)
1550  FORMAT( 20X,3(E15.7,10X),E15.7)
1500  CONTINJE
1501  CONTINUE
C
C        PLOT THE PRESSURE AMPLITUDE ALONG THE BOTTOM
C        OF THE WEDGE.
C
      QRHO12 = RHO12
      QC12 = C12
      QBETA = BETAD5
      QYIN = YINORM
      QPINC = Y2NORM / DFLOAT(N)
      NN = N + 1
C
C        SCALE AMPLITUDE FOR PLOTTING.
C
      DO 1505 IJK = 1,NN
      QPLOTA(IJK) = PA(IJK) * 0.5DO
      QNORM(IJK) = YNORM(IJK)
1505  CONTINUE
      CALL PLOTS(0,3,0)
      CALL AXISMR(QN3RM(1),QNORM(N+1),QXLAB(1),QYLAB(1),0,0)
      CALL CAPSHN(1)
      CALL AMPPLT(QNORM,QPLOTA,NN)
      CALL PLOT(0.,0.,-999)
      GO TO 100
C
C        INTEGRATION INTO THE BOTTOM
C
C
C        AN ATTENUATION COEFFICIENT (ALPHA) IS INCORPORATED
C        TO ANALYSE MODE INTERFERENCE EFFECTS.  WHEN ALPHA
C        IS ZERO, THE CALCULATIONS ARE UNATTENUATED.  THIS
C        OPTION IS NOT AVAILABLE IN ANGLE DOMAIN CALCULATIONS.
C
2000  CONTINJE
C
2100  READ(5,2100) ETABEG,ETAMAX,XI,INC
      FORMAT(3(F15.7,5X),I5)
2102  READ(5,2102) ALPHA
      FORMAT(F15.7)
      WRITE(6,2150) ETABEG,ETAMAX,INC,XI
2150  FORMAT(//15X,'DEPTH DOMAIN INPUT DATA',//
     *        25X,'BEGINNING ETA(Z/X)    ',10X,F5.2/
     *        25X,'MAXIMUM DEPTH ETA(Z/X) ',10X,F5.2/
     *        25X,'DEPTH INCREMENTS USED  ',7X,I5/
     *        25X,'Y/X DISTANCE FOR PROBE ',5X,F15.7/)
```

64

```
2103  WRITE(6,2103), ALPHA
      FORMAT(/,20X,'ALPHA =',5X,F15.7)
C
C        NOW SET UP CONSTANT TERMS FOR LATER USE AND INITIALIZE ETA.
C
      WN2X = PI / (2.0D0 * DSQRT(2.0D0 * DTAN(ANGLC) * DTAN(BETA))
      WNTRM = DSQRT(2.0D0 * WN2X / PI) / 4.0D0
      CPI = DCOS(0.75D0 * PI)
      SPI = DSIN(0.75D0 * PI)
C
C        NOW PREPARE TO INTEGRATE.  THE REAL AND IMAGINARY POTIONS
C        ARE DONE SEPARATELY.
C
      DXI = DY / (DFLOAT(N) * CAPX)
      ETAINC = (ETAMAX - ETABEG) / DFLOAT(INC)
      JJ = INC + 1
      DO 2500 KK = 1,JJ
C
C        CALCULATE THE INTEGRAL MULTIPLIERS
C
      ETA = DFLOAT(KK-1) * ETAINC
      PRETRM = ETA * WNTRM
      ETASQR = ETA**2.0D0
C
C        NOW CALCULATE THE AMPLITUDE TERM COMMON TO BOTH THE REAL AND
C        IMAGINARY INTEGRATIONS. XI PRIME IS THE QUANTITY YY FROM THE
C        BOTTOM DOMAIN CALCULATIONS.
C
      SUMRL = 0.0D0
      SUMIM = 0.0D0
      L = N + 1
      DO 2550 LL = 1,L
      IF(YNORM(LL).EQ.0.0D0.AND.ETASQR.EQ.0.0D0) GO TO 2540
      XIETA = ((XI - YNORM(LL))**2   + ETASQR)
C
C        THE AMPLITUDE MAY BE ATTENUATED.
C
      AMPTRM = PA(LL) * DEXP(-1.0 * ALPHA * DSQRT(XIETA))/
     *         (XIETA**0.75)
C
C        THE PHASE TERM IS ALSO A COMMON TERM TO BOTH INTEGRALS.
C
      PHSTRM = PH(LL) - (WN2X * DSQRT(XIETA))
C
C        NOW SUM OVER THE REAL AND IMAGINARY PARTS.
C
      COSPHS = DCOS(PHSTRM)
      SINPHS = DSIN(PHSTRM)
```

65

```
      CHIMRL = COSPHS * AMPTRM * DXI
      CHIMIM = SINPHS * AMPTRM * DXI
      GO TO 2545
2540  CONTINUE
      CHIMRL = 0.0D0
      CHIMIM = 0.0D0
2545  CONTINUE
      SUMRL = SUMRL + CHIMRL
      SUMIM = SUMIM + CHIMIM
2550  CONTINUE
      PARTR = PRETR4 * (CPI * SUMRL - SPI * SUMIM)
      PARTI = PRETR4 * (CPI * SUMIM + SPI * SUMRL)
      BTMDPH(KK) = ETA
      QETA(KK) = BT4DPH(KK)
      BTMAMP(KK) = DSQRT(PARTR**2    + PARTI**2 )
      IF( PARTI.EQ.0.0D0) GO TO 2546
      BTMPHS(KK) = DATAN2(PARTI,PARTR)
      GO TO 2500
2546  BTMPHS(KK) = 0.0D0
2500  CONTINUE
C
C        WRITE OUT THE RESULTS.
C
2600  WRITE(6,2600)
      FORMAT(1//20X,'Z DISTANCE',19X,'Z PRESSURE',12X,'PHASE ANGLE'///)
      DO 2700 MM = 1,JJ
      WRITE(6,2800) BTMDPH(MM),BTMAMP(MM),BTMPHS(MM)
2800  FORMAT( 20X,E15.7,10X,E15.7,10X,E15.7)
2700  CONTINUE
C
C        NOW PLOT THE PRESSURE AMPLITUDE INTO THE BOTTOM.
C
      IY = 1
      QETAB = ETABEG
      QETAM = ETAMAX
      CALL PLOT(0.,0.,-3)
      CALL AXISMR(QETAB,QETAM,QXLAB(2),QYLAB(2),0.,IY)
      CALL CAPSHN(2)
      SCALE = DSQRT(DABS(XI - 1.0D0))
      DO 2705 IL = 1,JJ
      QBAMP(IL) = BTMAMP(IL) * 2.0D0 * SCALE * 5.0D0/6.0D0
2705  CONTINUE
      CALL AMPPLT(QETA,QBAMP,JJ)
      CALL PLOT(0.,0.,-999)
      GO TO 100
3000  CONTINUE
C        THE FOLLOWING CODE CALCULATES THE PRESSURE AND AMPLITUDE
C        IN THE BOTTOM FOR A GIVEN CONSTANT SIGMA = (R/CAPX) AND
```

66

```
C       AS A FUNCTION OF ANGLE CAPITAL THETA (THETAK).
C
C       INPUT CONSISTS OF:
C       SIGMA = THE RADIUS NORMALIZED TO CAPX.
C       CTHBEG = THE BEGINNING ANGLE IN DEGREES.
C       CTHEND = THE ENDING ANGLE IN DEGREES
C       CTHINC = THE ANGULAR INCREMENT IN DEGREES, SHOULD NOT
C       BE LARGER THAN 0.5 DEGREES.
C
C       READ IN INPUT
C
 3100   READ(5,3100) SIGMA, CTHBEG, CTHEND, CTHINC
 3100   FORMAT(4(F5.2,5X))
        WRITE(6,3150) SIGMA, CTHBEG, CTHEND, CTHINC
 3150   FORMAT(//15X,'ANGLE DOMAIN INPUT DATA:'//
     *          25X,'SIGMA (R/X) =',10X,F5.2//
     *          25X,'BEG CAP THETA =',10X,F5.2//
     *          25X,'END CAP THETA =',10X,F5.2//
     *          25X,'CAP THETA INC =',10X,F5.2/)
C
C       NOW SET UP CONSTANT TERMS FOR LATER USE.
C
        RTHBEG = CTHBEG * PI / 180.0D0
        RTHEND = CTHEND * PI / 180.0D0
        RTHINC = CTHINC * PI / 180.0D0
        WN2X = PI/(2.0D0 * DTAN(ANGLC) * DTAN(BETA))
        WNTRM = DSQRT(2.0D0 * WN2X / PI) / 4.0D0
        CPI = DCOS(0.2500 * PI)
        SPI = DSIN(0.2500 * PI)
C
C       NOW PREPARE TO INTEGRATE. THE REAL AND IMAGINARY PORTIONS
C       ARE DONE SEPARATELY.
C
        DXI = DY / (DFLOAT(N) *CAPX)
        INC = IDINT((RTHEND - RTHBEG) / RTHINC)
        JJ = INC + 1
        DO 3500 KK = 1,JJ
C
C       CALCULATE THE INTEGRAL MULTIPLIERS.
C
        THETAK = RTHBEG + ((KK - 1) * RTHINC)
        EPSLON = SIGMA * DCOS(THETAK)
        TSIGMA = DSQRT((SIGMA**2) - (EPSLON**2))
        PRETRM = TSIG4A * WNTRM
        TSSQR = TSIGMA**2.0
C
C       NOW CALCULATE THE AMPLITUDE TERM COMMON TO BOTH THE REAL
C       AND IMAGINARY INTEGRATIONS. XI PRIME IS THE QUANTITY YY
```

67

```
C     FROM THE BOTTOM DOMAIN CALCULATIONS.
C
      SUMRL = 0.0D0
      SUMIM = 0.0D0
      L = N + 1
      DO 3550 LL = 1,L
      IF(YNORM(LL).EQ.(0.0D0).AND.TSSQR.EQ.(0.0D0)) GO TO 3540
      XI = 1.0D0 - EPSLON
      XITS = ((XI - YNORM(LL))**2 + TSSQR)
      AMPTRM = PA(LL) / (XITS**0.75)
C
C     THE PHASE TERM IS ALSO A COMMON TERM TO BOTH INTEGRALS.
C
      PHSTRM = PH(LL) - (WN2X * DSQRT(XITS))
C
C     NOW SUM OVER THE REAL AND IMAGINARY PARTS.
C
      COSPHS = DCOS(PHSTRM)
      SINPHS = DSIN(PHSTRM)
      CHIMRL = COSPHS * AMPTRM * DXI
      CHIMIM = SINPHS * AMPTRM * DXI
      GO TO 3545
 3540 CHIMRL = 0.0D0
      CHIMIM = 0.0D0
 3545 CONTINUE
      SUMRL = SUMRL + CHIMRL
      SUMIM = SUMIM + CHIMIM
 3550 CONTINUE
      PARTR = PRETR4 * (CPI * SUMRL - SPI * SUMIM)
      PARTI = PRETR4 * (CPI * SUMIM + SPI * SUMRL)
      BTMDPH(KK) = THETAK * 180.0D0 / PI
      QETA(KK) = BTMDPH(KK)
      BTMAMP(KK) = DSQRT((PARTR**2) + (PARTI**2) )
      IF(PARTI.EQ.0.0D0) GO TO 3555
      BTMPHS(KK) = DATAN2(PARTI,PARTR)
      GO TO 3560
 3555 BTMAMP(KK) = 0.0D0
 3560 CONTINJE
 3500 CONTINJE
C
C     NOW WRITE OJT THE RESULTS.
C
      WRITE(6,3600)
 3600 FORMAT(//20X,'ANGLE DOWN',19X,'R PRESSURE',12X,'PHASE ANGLE'//)
      DO 3700 MM = 1,JJ
      WRITE(6,3800) BTMDPH(MM),BTMAMP(MM),BTMPHS(MM)
 3800 FORMAT( 20X,E15.7,10X,E15.7,10X,E15.7)
 3700 CONTINUE
```

```
C          NOW PLOT THE AMPLITUDE AS A FUNCTION OF ANGLE
      IX = 1
      IY = 1
      CALL PLOT(0.,0.,-3)
      QBEG = CTHBEG
      QEND = CTHEND
      CALL AXISMR(QBEG,QEND,QXLAB(3),QYLAB(2),IX,IY)
      CALL CAPSHN(3)
      DO 3705 IL = 1,JJ
      QBAMP(IL) = BTHAMP(IL) * 2.0D0 * 5.0D0/6.0D0
3705  CONTINUE
      CALL AMPPLT(QETA,QBAMP,JJ)
      CALL PLOT(0.,0.,-999)
      GO TO 100
5000  CONTINUE
      CALL PLOTS(0.,0.,+999)
      STOP
      END
```

69

```
      SUBROUTINE PRESS(DISTX,PAMP,PHAS)

C     DEFINE CHARACTERISTICS OF VARIABLES, PARAMETERS, CONSTANTS

      IMPLICIT REAL*8(A-H,O-P,R-Z),REAL*4(Q),INTEGER(I-N)
      COMPLEX*16 R,RA,RB,REFL,REFLNO,P,PRES,Z
      COMMON C21,RC21,BETA,WN,PI,ANGLO,F,ANGLSO

C     INITIALIZE COMPLEX PRESSURE P = 0.0 + J0.0

      P = (0.0D0,0.0D0)

C     RESET COUNTER N=0, RESET IFLAG = 0.

      N = 0
      IFLAG = 0
   10 CONTINUE

C     CALCULATE ANGLN AND DETERMINE IF ANGLE IS IN THE RANGE OR NOT
C     IF ANGLN.GE.PAI GO TO THE NEXT STEP

      ANGLN = 2.0D0 * INT((N + 1.) / 2.) * BETA + (-1)**N * ANGLO
      IF (ANGLN.GE.PI) GO TO 80

C     CALCULATE THE TOTAL REFLECTION COEFFICIENT R BY EACH PATH

      IF(IFLAG.EQ.1) GO TO 40
      REFLNO = REFL(ANGLN)
      IF(N.GE.2) GO TO 20
      RA = REFLNO
      R = RA
      GO TO 30
   20 CONTINUE
      RA = RA * REFLNO
      R = RA
   30 CONTINUE
      IFLAG = 1
      GO TO 70
   40 CONTINUE
      REFLNO = REFL(ANGLN)
      IF (N.GE.2) GO TO 50
      RB = REFLNO
      R = RB
      GO TO 60
   50 CONTINUE
      RB = RB * REFLNO
      R = RB
   60 CONTINUE
```

70

```
         IFLAG = 0
  70  CONTINUE

C     CALCULATE PARAMETERS Z AND PRES
C
      Z=DCMPLX(0.0D0,WN * DISTX * DCOS(ANGLN))
      PRES=CDEXP(Z)*(-1)**INT((N+1.)/2.)*
     *     (1.0D0 + 1.0D0 / REFLNO) * R

C     CALCULATE THE PRESSURE WHICH IS THE SUM OVER PRES.
C
      P = P + PRES

C     SET TO THE NEXT PAIR OF IMAGES
C
      N = N + 1
      GO TO 10
  80  CONTINUE

C     CALCULATE PA AND PH, AND RETURN BACK TO THE MAIN ROUTINE.
C
      PAMP = CDABS(P)
      PREAL = DREAL(P)
      PIMAG = DIMAG(P)
      IF(PIMAG.EQ.0.3D0) GO TO 90
      PHAS = DATAN2(PIMAG,PREAL)
      GO TO 100
  90  PHAS = 0.0D0
 100  CONTINUE
      RETURN
      END
```

71

```
      FUNCTION REFL (ANGLN)

C     DEFINE CHARACTERS OF VARIABLES, PARAMETERS AND CONSTANTS
C
C
      IMPLICIT REAL*8(A-H,O-P,R-Z),REAL*4(Q),INTEGER(I-N)
      COMPLEX*16 PSAI,REFL
      COMMON C21,RC21,BETA,WN,PI,ANGLO,F,ANGLSO

C     CALCULATE PARAMETER CHECK
C
      CHECK = 1.0D0 - C21**2 * DCOS(ANGLN)**2

C     IDENTIFY THE GRAZING ANGLE AND CHECK TO SEE IF IT IS LESS
C     THAN THE CRITICAL ANGLE.
C
      IF (CHECK.GT.0.0D0) GO TO 10

C     CALCULATE THE PARAMETER PSAI FO THE REFLECTION COEFFICIENT
C     OF EACH BOUNCE.   THERE ARE TWO WAYS WHICH DEPEND ON THE
C     IDENTIFICATION OF A CHECK.
C
      PSAI = DCMPLX(0.0D0,-DSQRT(-CHECK)/DSIN(ANGLN))
      GO TO 20
   10 CONTINUE
      PSAI = DCMPLX(DSQRT(CHECK)/DSIN(ANGLN),0.0D0)
   20 CONTINUE

C     CALCULATE REFL
C
      REFL = (RC21 - PSAI) / (RC21 + PSAI)

C     RETURN BACK TO SUBROUTINE PRESS
C
      RETURN
      END
```

72

```
      SUBROUTINE AXISMR(QSTR,QFIN,QXLAB,QYLAB,IX,IY)

C     THIS SUBROUTINE DRAWS THE AXES AND WRITES THE SCALE
C     MARKINGS EVERY ONE-FOURTH ETA.  THE VERTICAL SCALE
C     IS FIXED SO VARIOUS RUNS CAN BE OVERLAID.

C     FIRST DRAW A BOX SIX INCHES LONG BY FIVE INCHES HIGH.
C     THE BOX IS OFFSET TO ALLOW FOR LABELING.

      CALL OFFSET(-1.,-1.,-1.,1.)
      CALL NEWPEN(3)
      CALL PLOT(0.,0.,+13)
      CALL PLOT(6.,0.,+12)
      CALL PLOT(6.,5.,+12)
      CALL PLOT(0.,5.,+12)
      CALL PLOT(0.,0.,+12)
      IF(IX.EQ.1) GO TO 150

C     NOW LABEL THE X-AXIS EVERY ONE-FOURTH UNIT.

      QSTEP = ABS(6.0 / ((QFIN - QSTR) * 4.0) )
      QMARK = QSTEP
      QTICK = QSTR + 0.25
100   CONTINUE
      CALL NEWPEN(1)
      CALL PLOT(QMARK,0.,+13)
      CALL PLOT(QMARK,-0.1,+12)
      CALL NUMBER(QMARK+0.85,0.8,0.07,QTICK,0.0,+2)
      QMARK = QMARK + QSTEP
      QTICK = QTICK + 0.25
      IF(QMARK.LT.6.0) GO TO 100
      GO TO 170
150   CONTINUE

C     MARK THE AXIS FOR ANGLE DOMAIN

      QSTEP = ABS(6.0 * 5.0 /(QFIN -QSTR) )
      QMARK = QSTEP
      QTICK = QSTR + 5.0
160   CONTINUE
      CALL NEWPEN(1)
      CALL PLOT(QMARK,0.0,+13)
      CALL PLOT(QMARK,-0.1,+12)
      CALL NUMBER(QMARK+0.85,0.8,0.07,QTICK,0.0,+2)
      QMARK = QMARK + QSTEP
      QTICK = QTICK + 5.0
      IF(QMARK.LT.6.0) GO TO 160
170   CONTINUE
```

73

```
C     NOW MARK THE Y-AXIS, ONE UNIT FOR EVERY TWO INCHES
C     IF THIS IS FOR THE WEDGE BOTTOM.

      IF(IY.EQ.1) GO TO 300
      QYSTEP = 1.0
      QYVAL = 2.0
      DO 200 I = 1,4
      CALL PLOT(0.0,QYSTEP-1.0,+13)
      CALL PLOT(-0.1,QYSTEP-1.0,+12)
      CALL NUMBER(0.7,QYSTEP,0.07,QYVAL,0.0,+1)
      QYSTEP = QYSTEP + 1.0
      QYVAL = QYVAL + 2.0
  200 CONTINUE
      GO TO 400
  300 CONTINUE

C     MARK THE AXIS FOR BOTTOM AMPLITUDE.

      QYY = 5.0 / 6.0
      QYINC = QYY
      QYYVAL = 0.5
      DO 350 J = 1,5
      CALL PLOT(-0.1,QYY,+13)
      CALL PLOT(0.0,QYY,+12)
      CALL NUMBER(-0.5,QYY+1.0,0.0.07,QYYVAL,0.0,+1)
      QYY = QYY + QYINC
      QYYVAL = QYYVAL + 0.5
  350 CONTINUE
  400 CONTINUE

C     FINALLY PRINT LABELS ON X AND Y AXES.

      CALL SYMBOL(3.5,0.25,0.14,QXLAB,0.0,4)
      CALL SYMBOL(4.5,0.25,0.14,QLAB,0.0,-1)
      CALL SYMBOL(0.3,3.0,0.14,QYLAB,90,-1)
      CALL SYMBOL(0.3,4.0,0.14,62,0.0,-1)
      RETURN
      END
```

74

```fortran
      SUBROUTINE CAPSHN(ITYP)
C     THIS SUBROUTINE PRINTS PERTINANT DATA ABOUT THE RUN, SUCH AS
C     SOURCE ANGLE, WEDGE ANGLE, ETC. ON THE VARIAN PLOT
C
      IMPLICIT REAL*8(A-H,O-P,R-Z),REAL*4(Q),INTEGER(I-N)
      DIMENSION PA(1001),PH(1001),YY(1001),HOFXI(1001),
     *BTMDPH(1001),BTMAMP(1001),BTMPHS(1001),YNORM(1001),
     **QXLAB(3),QYLAB(2),QPLOTA(1001),QNDR4(1001),QBAMP(1001),
     *QBETA(1001)
      COMMON C21,RC21,BETA,WN,PI,ANGLO,F,ANGLSO
      COMMON /FINE/SRCDIS,RD1,RO2,C1,C2,BETADG,YINORM,Y2NORM,
     *C12,RHO12,PIN,PA,PH,YY,YNORM,DY,ANGLC,CAPX,N
      COMMON /ANGLE/SIGMA,CTHBEG,CTHEND,CTHINC
      COMMON /BTM/ETABEG,ETAMAX,XI,INC
      CALL PLOT(0.,0.,+13)
      CALL NEWPEN(1)
      CALL SYMBOL(1.25,10.0,0.07,4HRHO1,0.0,4)
      QRHO1 = RO1
      CALL NUMBER(2.5,10.0,0.07,QRHO1,0.0,+4)
      CALL SYMBOL(1.25,9.75,0.07,4HRHO2,0.0,4)
      QRHO2 = RO2
      CALL NUMBER(2.5,9.75,0.07,QRHO2,0.0,+4)
      CALL SYMBOL(1.25,9.50,0.07,4HRRAT,0.0,4)
      QRHI2 = RHO12
      CALL NUMBER(2.5,9.50,0.07,QRHI2,0.0,+4)
      CALL SYMBOL(1.25,9.25,0.07,4HC1  ,0.0,4)
      QC1 = C1
      CALL NUMBER(2.5,9.25,0.07,QC1,0.0,+4)
      CALL SYMBOL(1.25,9.00,0.07,4HC2  ,0.0,4)
      QC2 = C2
      CALL NUMBER(2.5,9.00,0.07,QC2,0.0,+4)
      CALL SYMBOL(1.25,8.75,0.07,4HCRAT,0.0,4)
      QC12 = C12
      CALL NUMBER(2.5,8.75,0.07,QC12,0.0,+4)
      CALL SYMBOL(1.25,8.50,0.07,4HBETA,0.0,4)
      QBETA = BETADG
      CALL NUMBER(2.5,8.50,0.07,QBETA,0.0,+2)
      CALL SYMBOL(1.25,8.25,0.07,4HSRCA,0.0,4)
      QANG = ANGLSO
      CALL NUMBER(2.5,8.25,0.07,QANG,0.0,+2)
      CALL SYMBOL(1.25,8.00,0.07,4HSRCD,0.0,4)
      QDIS = SRCDIS
      IF(QDIS.EQ.0.0) QDIS = 999.
      CALL NUMBER(2.5,8.00,0.07,QDIS,0.0,+2)
      CALL SYMBOL(1.25,7.75,0.07,4HWINC,0.0,4)
      QINC = Y2NORM / DFLOAT(N)
      CALL NUMBER(2.5,7.75,0.07,QINC,0.0,+3)
```

75

```
C     ITYPE = 1 IMPLIED WEDGE AMP PLOT
C     ITYPE = 2 IMPLIES  DEPTH DOMAIN
C     ITYPE = 3 IMPLIES  ANGLE DOMAIN

      IF(ITYP.EQ.1) GO TO 1000
      IF(ITYP.EQ.3) GO TO 100
      QBEG = ETABEG
      CALL SYMBOL(4.0,10.0,0.07,4HEBEG,0.0,4)
      CALL NUMBER(5.0,10.0,0.07,QBEG,0.0,+1)
      CALL SYMBOL(4.0,9.75,0.07,4HEEND,0.0,4)
      QEND = ETAMAX
      CALL NUMBER(5.0,9.75,0.07,QEND,0.0,+1)
      CALL SYMBOL(4.0,9.50,0.07,4HEINC,0.0,4)
      QINC = INC
      CALL NUMBER(5.0,9.50,0.07,QINC,0.0,0)
      CALL SYMBOL(4.0,9.25,0.07,4HFPNT,0.0,4)
      QXI = XI
      CALL NUMBER(5.0,9.25,0.07,QXI,0.0,+2)
      GO TO 1000
  100 CONTINUE
      CALL SYMBOL(4.0,10.0,0.07,4HSGMA,0.0,4)
      QSIG = SIGMA
      CALL NUMBER(5.0,10.0,0.07,QSIG,0.0,+2)
      CALL SYMBOL(4.0,9.75,0.07,4HTBEG,0.0,4)
      QBEG = CTHBEG
      CALL NUMBER(5.0,9.75,0.07,QBEG,0.0,+2)
      CALL SYMBOL(4.0,9.50,0.07,4HTEND,0.0,4)
      QEND = CTHEND
      CALL NUMBER(5.0,9.50,0.07,QEND,0.0,+2)
      CALL SYMBOL(4.0,9.25,0.07,4HTINC,0.0,4)
      QINC = CTHINC
      CALL NUMBER(5.0,9.25,0.07,QINC,0.0,+3)
 1000 CONTINJE
      RETURN
      END
```

```
      SUBROUTINE AMPPLT(QXAXIS,QYVAL,INCR)
      DIMENSION QXAXIS(1001),QYVAL(1801)
      QXSCAL = 6.0 / (QXAXIS(INCR) - QXAXIS(1))
      CALL PLOT(0.,0.,+13)
      CALL NEWPEN(3)
      DO 100 II = 1,INCR
      QXVAL = (QXAXIS(II) - QXAXIS(1)) * QXSCAL
      CALL PLOT(QXVAL,QYVAL(II),+12)
100   CONTINUE
      RETURN
      END
```

77

```
      SUBROUTINE FINESR
      IMPLICIT REAL*8(A-H,O-P,R-Z),REAL*4(Q),INTEGER(I-N)
      DIMENSION PA(1001),PH(1001),YY(1001),YNORM(1001),HOFXI(1001)
      COMMON C21,RC21,BETA,WN,PI,ANGLO,F,ANGLSO
      COMMON /FINE/SRCDIS,RO1,RO2,C1,C2,BETADG,Y1NORM,Y2NORM,
     * C12,RHO12,PINC,PA,PH,YY,YNORM,DY,ANGLC,CAPX,N

      ANGLC = DARCOS (C1/C2)
      HO = C1 / (4.0D0 *F* DSIN(ANGLC))
      CAPX = HO / DSIN(BETA)
      SRCDIS = SRCDIS * CAPX

C
C     BETA CAN BE GENERALIZED TO ANGLESO  IN RADIANS
      SRCDPH = SRCDIS * DSIN (BETA / 2.0D0)
      Y1 = Y1NORM * CAPX
      Y2 = Y2NORM * CAPX
      WRITE(6,1000) C1,C2,RO1,RO2,BETA,BETADG,SRCDIS,
     * SRCDPH,Y1NORM,Y1,Y2NORM,Y2,HO,CAPX
1000  FORMAT(//25X,'FINITE SOURCE INPUT DATA'//
     * 15X,'C1=',10X,F15.7,5X,'C2=',9X,F15.7/
     * 15X,'RO1=',8X,F15.7,5X,'RHO2=',7X,F15.7/
     * 15X,'BETARAD=',5X,F15.7,5X,'BETADG=',5X,F15.7/
     * 15X,'SOURCE DIS=',2X,F15.7,5X,'SOURCE DPH=',1X,F15.7/
     * 15X,'Y1NORM=',6X,F15.7,5X,'Y1=',9X,F15.7/
     * 15X,'Y2NORM=',6X,F15.7,5X,'Y2=',9X,F15.7/
     * 15X,'CUT-OFF DPH=',1X,F15.7,5X,'CAPX=',8X,F15.7//)

      DY = Y2 - Y1
      PI = 4.0D0 * DATAN(1.0D0)
      WN = 2.0D0 * PI * F / C1
      C21 = C2/ C1
      RC21 = C2 * RO2 / (C1 * RO1)
      C12 = C1/ C2
      RHO12 = RO1 / RO2
      PINC = 1.0D0 / DFLOAT(N)

      ANGLO = BETA - DARSIN(SRCDPH/SRCDIS)
      WRITE(6,2000)
2000  FORMAT(//22X,'DISTANCE',17X,'NORMALIZED DIST',9X,
     * 'PRESSURE AMP.',12X,'PHASE ANGLE'//)

      L = N + 1
      DO 3000 I = 1,L
      YY(I) = Y1 + DFLOAT(I-1) * DY * PINC
      DISTY = YY(I) / SRCDIS
      CALL FINPR(DISTY,PAMP,PHAS,SRCDIS,SRCDPH)
      PA(I) = PAMP
      PH(I) = PHAS
      YNORM(I) = YY(I) / CAPX
      WRITE(6,4000) YY(I),YNORM(I),PA(I),PH(I)
```

```
4000 FORMAT( 20X,3(F15.7,10X),F15.7)
3000 CONTINUE
     RETURN
     END
```

```fortran
      SUBROUTINE FINPR(DISTY,PAMP,PHAS,SRCDIS,SRCDPH)
      IMPLICIT REAL*8(A-H,O-P,R-Z),REAL*4(Q),INTEGER(I-N)
      COMPLEX*16 PSAI,REFL,REFLNO,R,Z,PRES,P
      COMMON C21,RC21,BETA,WN,PI,ANGLO,F,ANGLSO
      P = (0.0D0,0.0D0)
      N = 0
   10 CONTINUE
      ANGLN = 2.0D0 * INT((N + 1.)/2.) * BETA +
     *        (-1)**N*ANGLO
      IF(ANGLN.GE.PI) GO TO 50
      DD = DCOS(ANGLN) - DISTY
      THETAO = DATAN2(DSIN(ANGLN),DD)
      DR = DSQRT(1.0D0 + DISTY**2 - 2.0D0 * DISTY * DCOS(ANGLN))
      R = (1.0D0,0.0D0)
      MM = IDINT(ANGLN/(2.0D0 * BETA))
      L = MM + 1
      DO 40 M = 1,L
      THETAM = THETAO - 2.0D0 * DFLOAT(M-1) * BETA
      CHECK = 1.0D0 - C21**2 * DCOS(THETAM)**2
      IF(CHECK.GT.0.0D0) GO TO 20
      PSAI = DCMPLX(0.0D0,-DSQRT(-CHECK)/DSIN(THETAM))
      GO TO 30
   20 CONTINUE
      PSAI = DCMPLX(DSQRT(CHECK)/DSIN(THETAM),0.0D0)
   30 CONTINUE
      REFL = (RC21 - PSAI) / (RC21 + PSAI)
      IF(M.EQ.1) REFLNO = REFL
      R = R * REFL
   40 CONTINUE
      Z = DCMPLX(0.0D0,-WN * SRCDIS * DR)
      DIRET = 1.0D0
      PRES = DIRET * CDEXP(Z) * (-1.)**INT((N + 1.)/2.) *
     *       (1.0D0 + 1.0D0/REFLNO) ** R / DR
      P = P + PRES
      N = N + 1
      GO TO 10
   50 CONTINUE
      PAMP = CDABS(P)
      PREAL = DREAL(P)
      PIMAG = DIMAG(P)
      PHAS = DATAN2(PIMAG,PREAL)
      RETURN
      END
```

80

LIST OF REFERENCES

1. Tien, P. K., and Martin, R. J., "Experiments on Light Waves in a Thin Tapered Film and a New Light-Wave Coupler", *Applied Physics Letters*, v. 18, p. 398-401, 1 May 71.

2. Kuznetsov, V. K., "Emergence of Normal Modes Propagating in a wedge on a Half-space from the former into the Latter", *Soviet Physical Acoustics*, v. 19, p. 241-245, Nov. - Dec. 1973.

3. Tien, P. K., Smolinsky, G., and Martin, R. J., "Radiation Fields of a Tapered Film and a Novel Film-to-Fiber Coupler", *Transactions on Microwave Theory and Techniques*, v. MTT-23, p. 79-85, January 1975.

4. University of Washington Technical Report 209, *Ocean-Earth Acoustic Coupling*, by Sigelman, R. A., et.al., May 1978.

5. Kawamura, M. and Ioannou, I., *Pressure on the Interface Between a Converging Fluid Wedge and a Fast Fluid Bottom*, M. S. Thesis, Naval Postgraduate School, Monterey, CA. 1978.

6. Coppens, A., Notes on Sound Propagation in a Fast Bottom, (Informal).

7. Butkov, E., *Mathematical Physics*, p. 616, Addison-Wesley Publishing Company, 1968.

8. Netzorg, G. B., *Sound Transmission From a Tapered Fluid Layer into a Fast Bottom*, M. S. Thesis, Naval Postgraduate School, Monterey, CA, 1977.

9. Jensen, F. B., and Kuperman, W. A., "Sound Propagation in a Wedge-Shaped Ocean with a Penetrable Bottom", *Journal of the Acoustical Society of America*, v. 67, p. 1564-1566, May 1980.

10. Sanders, J., *The Experiment: Transmission of Acoustic Waves into a Fast Fluid Bottom from a Converging Fluid Wedge*, paper presented at the Workshop on Seismic Propagation in Shallow Water, Arlington, VA, 6-7 July 1978.

INITIAL DISTRIBUTION LIST

		No. Copies
1.	Defense Technical Information Center Cameron Station Alexandria, Virginia 22314	2
2.	Library, Code 0142 Naval Postgraduate School Monterey, California 93940	2
3.	Department Library Code 61 Department of Physics and Chemistry Naval Postgraduate School Monterey, California 93940	2
4.	Department Chairman, Code 61 Department of Physics and Chemistry Naval Postgraduate School Monterey, California 93940	1
5.	Mr. Robert F. Obrochta Earth and Ionispheric Program Code 464 800 N. Quincy St. Arlington, Virginia 22217	1
6.	Dr. W. A. Kuperman SACLANT ASW Research Centre APO New York 09019	1
7.	Dr. A. B. Coppens, Code 61Cz Department of Physics and Chemistry Naval Postgraduate School Monterey, California 93940	1
8.	Dr. J. V. Sanders, 61Sd Department of Physics and Chemistry Naval Postgraduate School Monterey, California 93940	1
9.	LCDR Norine A. Bradshaw 99 Corona Rd. Carmel, California 93923	1
10.	Dr. David Blackstock Applied Research Laboratories The University of Texas at Austin Post Office Box 8029 Austin, Texas 78712	1